

Hybrid deep additive neural networks

Gyu Min Kim and Jeong Min Jeon

Department of Statistics, Seoul National University, South Korea

Department of Data Science, Ewha Womans University, South Korea

Abstract: Traditional neural networks (multi-layer perceptrons) have become an important tool in data science due to their success across a wide range of tasks. However, their performance is sometimes unsatisfactory, and they often require a large number of parameters, primarily due to their reliance on the linear combination structure. Meanwhile, additive regression has been a popular alternative to linear regression in statistics. In this work, we introduce novel deep neural networks that incorporate the idea of additive regression. Our neural networks share architectural similarities with Kolmogorov-Arnold networks but are based on simpler yet flexible activation and basis functions. Additionally, we introduce several hybrid neural networks that combine this architecture with that of traditional neural networks. We derive their universal approximation properties and demonstrate their effectiveness through simulation studies and a real-data application. The numerical results indicate that our neural networks generally achieve much better performance than the traditional neural networks while using fewer parameters.

Keywords: Additive model, Basis expansion, Deep learning, Neural network

1 Introduction

Additive regression is a statistical modeling approach developed to capture nonlinear relationships between the responses and predictors without relying on strict assumptions on the form of these relationships. Instead of assuming a linear relationship, additive models allow the response variable to depend on the sum of smooth and potentially nonlinear functions of each predictor variable. There have been a number of methods to estimate additive models, such as methods based on kernel smoothing (e.g., [Linton and Nielsen \(1995\)](#), [Opsomer and Ruppert \(1997\)](#), [Mammen et al. \(1999\)](#), [Jeon and Park \(2020\)](#), [Jeon et al. \(2022\)](#)) and methods based on basis expansions (e.g., [Bilodeau \(1992\)](#), [Meier et al. \(2009\)](#), [Sardy and Ma \(2024\)](#)).

On the other hand, neural networks are becoming an important method in regression analysis. Its good practical performance and nice theoretical properties have been investigated by numerous works (e.g., [LeCun et al. \(2015\)](#), [Schmidhuber \(2015\)](#), [Bauer and Kohler \(2019\)](#), [Schmidt-Hieber](#)

(2020), Kohler and Langer (2021)). However, traditional neural networks (multi-layer perceptrons) sometimes struggle with capturing complex nonlinear relationships between predictors and responses. Additionally, they often require a huge number of parameters, which leads to high computational and memory demands. These issues mainly come from that each node does not have sufficient nonlinearity.

Recently, several modifications using nonlinear basis functions have been proposed to overcome this issue. For example, Fakhoury et al. (2022) proposed an approach that uses a B-spline basis expansion, instead of the composition of an activation function and an affine function, to construct each node. However, this work considered only one hidden layer. Horowitz and Mammen (2007) introduced a deep version of this neural network and suggested to use B-splines or smoothing splines to estimate their neural network. However, this work mainly focused on deriving asymptotic error rates with arbitrary estimators satisfying certain conditions. Recently, Liu et al. (2024) proposed Kolmogorov-Arnold networks that have the same architecture as Horowitz and Mammen (2007). This approach uses a linear combination of the sigmoid linear unit function and a B-spline basis expansion to form each node. Although Liu et al. (2024) demonstrates fair performance, it requires high computational cost, resulting in a long training time. Additionally, it is complicated to implement and is prone to overfitting. Moreover, its universal approximation theorem holds only for a certain class of smooth functions.

In this work, we propose an alternative approach to Liu et al. (2024). Specifically,

- We propose a deep neural network that uses fixed activation functions and simple yet flexible basis functions, which make computation and implementation easy.
- We introduce hybrid neural networks that combine the above neural network and the traditional neural networks, which effectively avoid overfitting.
- We derive their universal approximation properties that hold for any continuous functions.

This paper is organized as follows. In Section 2, we introduce a neural network, named as a deep additive neural network (DANN), and its property. We also introduce its hybrid variants in Section 3. Section 4 contains simulation studies and Section 5 presents real data analysis. These numerical studies show that our neural networks have better performance than the traditional neural networks in terms of both prediction errors and numbers of parameters. Section 6 contains conclusions, and all technical proofs are provided in the Appendix.

2 Deep Additive Neural Networks

Let $Y \in \mathbb{R}$ be a response and $\mathbf{X} = (X_1, \dots, X_d)^\top \in [0, 1]^d$ for $d \geq 1$ be a vector of predictors. The traditional neural networks with single hidden layer assume that

$$(2.1) \quad \mathbb{E}(Y|\mathbf{X}) = \sum_{k=1}^p w_k \sigma \left(\sum_{j=1}^d w_{jk} X_j + b_k \right),$$

where $p \geq 1$ is the number of nodes in the hidden layer, $\sigma : \mathbb{R} \rightarrow \mathbb{R}$ is a non-polynomial continuous function, called an activation function, and $w_k, w_{jk}, b_k \in \mathbb{R}$ are parameters. The well-known universal approximation theorem (Cybenko (1989)) tells that, for any given continuous function $f : [0, 1]^d \rightarrow \mathbb{R}$ and constant $\epsilon > 0$, there exist $p \geq 1$ and $w_k, w_{jk}, b_k \in \mathbb{R}$ such that

$$\sup_{\mathbf{x}=(x_1, \dots, x_d)^\top \in [0, 1]^d} \left| f(\mathbf{x}) - \sum_{k=1}^p w_k \sigma \left(\sum_{j=1}^d w_{jk} x_j + b_k \right) \right| < \epsilon.$$

In spite of this nice property, it has been known that the practical performance of (2.1) is not good enough, particularly when the target regression function $\mathbb{E}(Y|\mathbf{X} = \cdot)$ is highly nonlinear, because σ is the only nonlinear function in (2.1).

To overcome this issue, we may replace the linear functions in (2.1) by nonlinear functions. Specifically, we consider the model

$$(2.2) \quad \mathbb{E}(Y|\mathbf{X}) = \sum_{k=1}^p f_k \left(\sum_{j=1}^d f_{jk}(X_j) \right),$$

where $f_k : \mathbb{R} \rightarrow \mathbb{R}$ and $f_{jk} : [0, 1] \rightarrow \mathbb{R}$ are possibly nonlinear functions. When $p = 1$ and f_1 is the identity function, this model reduces to the standard additive model. By taking appropriate f_k and f_{jk} , (2.2) may approximate highly nonlinear $\mathbb{E}(Y|\mathbf{X} = \cdot)$ better than (2.1) in practice. In fact, Kolmogorov's superposition theorem (Kolmogorov (1957)) says that any continuous function $f : [0, 1]^d \rightarrow \mathbb{R}$ can be written as $\sum_{k=1}^p \phi_k^f(\sum_{j=1}^d \phi_{jk}^f(x_j))$ for some $p \geq 1$ and continuous functions $\phi_k^f : \mathbb{R} \rightarrow \mathbb{R}$ and $\phi_{jk}^f : [0, 1] \rightarrow \mathbb{R}$. In this work, we take f_k and f_{jk} that can well approximate unknown ϕ_k^m and ϕ_{jk}^m , where $m := \mathbb{E}(Y|\mathbf{X} = \cdot)$. For this, we introduce a lemma.

Lemma 1. *There exists a set $\{B_r : [0, 1] \rightarrow \mathbb{R} \mid r \geq 1\}$ of known functions such that, for any given continuous function $\phi : [0, 1] \rightarrow \mathbb{R}$ and constant $\epsilon > 0$, there exist $q \geq 1$ and $c_r, c \in \mathbb{R}$ such that*

$$\sup_{x \in [0, 1]} \left| \phi(x) - \left(\sum_{r=1}^q c_r B_r(x) + c \right) \right| < \epsilon.$$

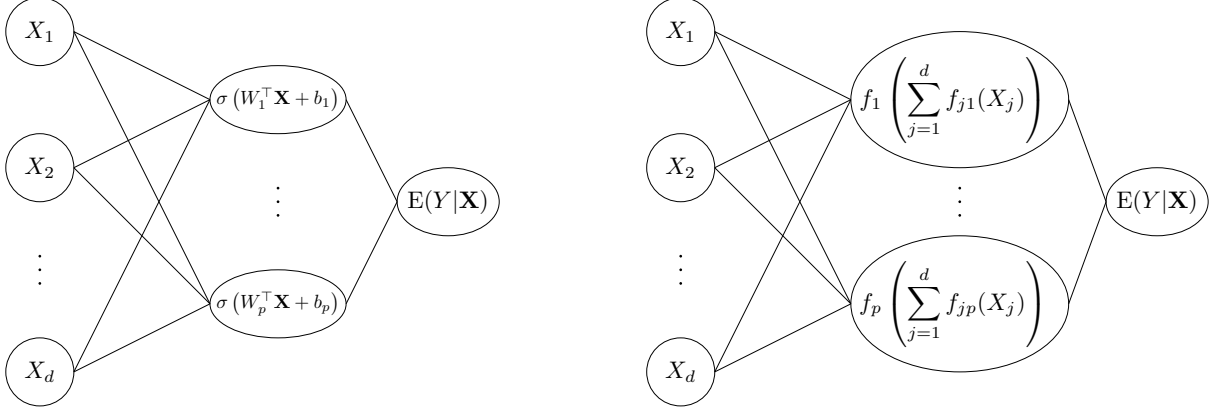


Figure 1: Architectures of (2.1) (left) and (2.2) (right). In the left panel, W_k denotes $(w_{1k}, \dots, w_{dk})^\top \in \mathbb{R}^d$.

For example, $\{B_r(x) : r \geq 1\} = \{x^r : r \geq 1\}$, $\{B_r(x) : r \geq 1\} = \{\cos(r\pi x) : r \geq 1\}$ and the Haar system on $[0, 1]$ (e.g., Haar (1910)), among many others, have the above property; see the proof of Lemma 1. In this work, we call B_r satisfying the property of Lemma 1 basis functions. From this,

$$\sum_{j=1}^d \phi_{jk}^m(x_j)$$

can be well approximated by

$$\sum_{j=1}^d \sum_{r=1}^{q_{jk}} c_{jkr} B_{jkr}(x_j) + b_k$$

for some $q_{jk} \geq 1$ and $c_{jkr}, b_k \in \mathbb{R}$, and any possibly different sets $\{B_{1kr} : r \geq 1\}, \dots, \{B_{dkr} : r \geq 1\}$ of basis functions. We also approximate $\phi_k^m : \mathbb{R} \rightarrow \mathbb{R}$ by the function

$$\sum_{\ell=1}^{q_k} c_{k\ell} B_{k\ell}(g(\cdot)) + b,$$

where $q_k \geq 1$, $c_{k\ell}, b \in \mathbb{R}$, $\{B_{k\ell} : \ell \geq 1\}$ is a set of basis functions, and $g : \mathbb{R} \rightarrow [0, 1]$ is a function. We call the model

$$(2.3) \quad \mathbb{E}(Y|\mathbf{X}) = \sum_{k=1}^p \sum_{\ell=1}^{q_k} c_{k\ell} B_{k\ell} \left(g \left(\sum_{j=1}^d \sum_{r=1}^{q_{jk}} c_{jkr} B_{jkr}(X_j) + b_k \right) \right) + b$$

an Additive Neural Network (ANN). Figure 2 illustrates the architecture of ANN. The following theorem shows that the ANN is a reasonable model.

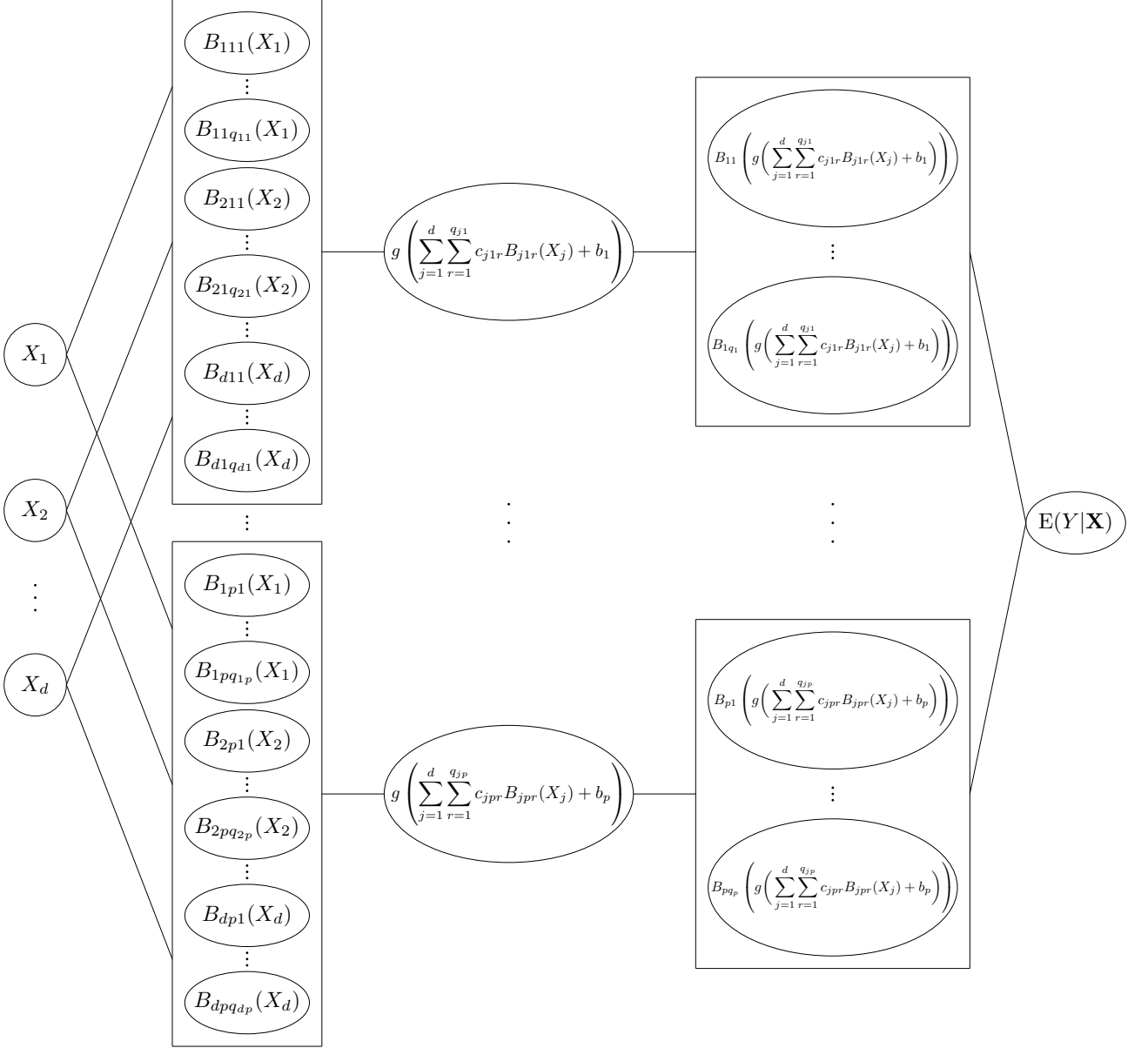


Figure 2: Architecture of ANN model.

Theorem 1. Let $\{B_{k\ell} : \ell \geq 1\}$ and $\{B_{jkr} : r \geq 1\}$ be any sets of basis functions and g be non-constant and Lipschitz continuous. Then, for any given continuous function $f : [0, 1]^d \rightarrow \mathbb{R}$ and constant $\epsilon > 0$, there exist $p, q_k, q_{jk} \geq 1$ and $c_{k\ell}, c_{jkr}, b_k, b \in \mathbb{R}$ such that

$$\sup_{\mathbf{x} \in [0, 1]^d} \left| f(\mathbf{x}) - \left(\sum_{k=1}^p \sum_{\ell=1}^{q_k} c_{k\ell} B_{k\ell} \left(g \left(\sum_{j=1}^d \sum_{r=1}^{q_{jk}} c_{jkr} B_{jkr}(x_j) + b_k \right) \right) + b \right) \right| < \epsilon.$$

Examples of g satisfying the assumption in Theorem 1 include the logistic function, $(\tanh + 1)/2$ and any Lipschitz continuous cumulative distribution function, where \tanh is the hyperbolic tangent function. The hyperparameters of ANN that we need to choose include p, q_k, q_{jk}, g and the sets of

basis functions. For given hyperparameters, we estimate $c_{k\ell}$, c_{jkr} , b_k and b in (2.3) by finding values that minimize $\sum_{i=1}^n (Y_i - \hat{Y}_i)^2$. For this, we initialize them and then update subsequently using an optimization algorithm.

Remark 1. *The ANN has important advantages.*

1. *First, the ANN architecture is easy to build. Note that $\{B_{jkr}(X_j) : 1 \leq j \leq d, 1 \leq r \leq q_{jk}\}$ for $1 \leq k \leq p$ that are in the left rectangles of Figure 2 can be easily obtained from \mathbf{X} . Similarly, $\{B_{k\ell}(g(\sum_{j=1}^d \sum_{r=1}^{q_{jk}} c_{jkr} B_{jkr}(X_j) + b_k)) : 1 \leq \ell \leq q_k\}$ that is in the k th right rectangle of Figure 2 can be easily obtained from $g(\sum_{j=1}^d \sum_{r=1}^{q_{jk}} c_{jkr} B_{jkr}(X_j) + b_k)$ for $1 \leq k \leq p$. If we use the same basis set, say $\{B_r : r \geq 1\}$, and the same number of basis functions, say q , across all nodes, then the ANN architecture is even more simplified; see Figure 3.*
2. *Second, we can directly apply optimization algorithms used for the traditional neural networks, such as ADAM (Kingma and Ba (2017)), to update the parameters of ANN. This is because $\sum_{j=1}^d \sum_{r=1}^{q_{jk}} c_{jkr} B_{jkr}(X_j) + b_k$ is simply the linear combination of $\{B_{jkr}(X_j) : 1 \leq j \leq d, 1 \leq r \leq q_{jk}\} \cup \{1\}$ for $1 \leq k \leq p$, and*

$$\sum_{k=1}^p \sum_{\ell=1}^{q_k} c_{k\ell} B_{k\ell} \left(g \left(\sum_{j=1}^d \sum_{r=1}^{q_{jk}} c_{jkr} B_{jkr}(X_j) + b_k \right) \right) + b$$

is simply the linear combination of $\{B_{k\ell}(g(\sum_{j=1}^d \sum_{r=1}^{q_{jk}} c_{jkr} B_{jkr}(X_j) + b_k)) : 1 \leq k \leq p, 1 \leq \ell \leq q_k\} \cup \{1\}$.

3. *Cosine basis might approximate a periodic function well and the Haar basis might approximate a non-smooth function well. By mixing various types of basis, the ANN might approximate diverse functions well in practice.*

It has been known that the traditional neural networks with multiple hidden layers, sometimes called a Deep Neural Network (DNN), tends to provide better performance than that with single hidden layer. This motivates us to add more hidden layers to the ANN. The ANN with L hidden

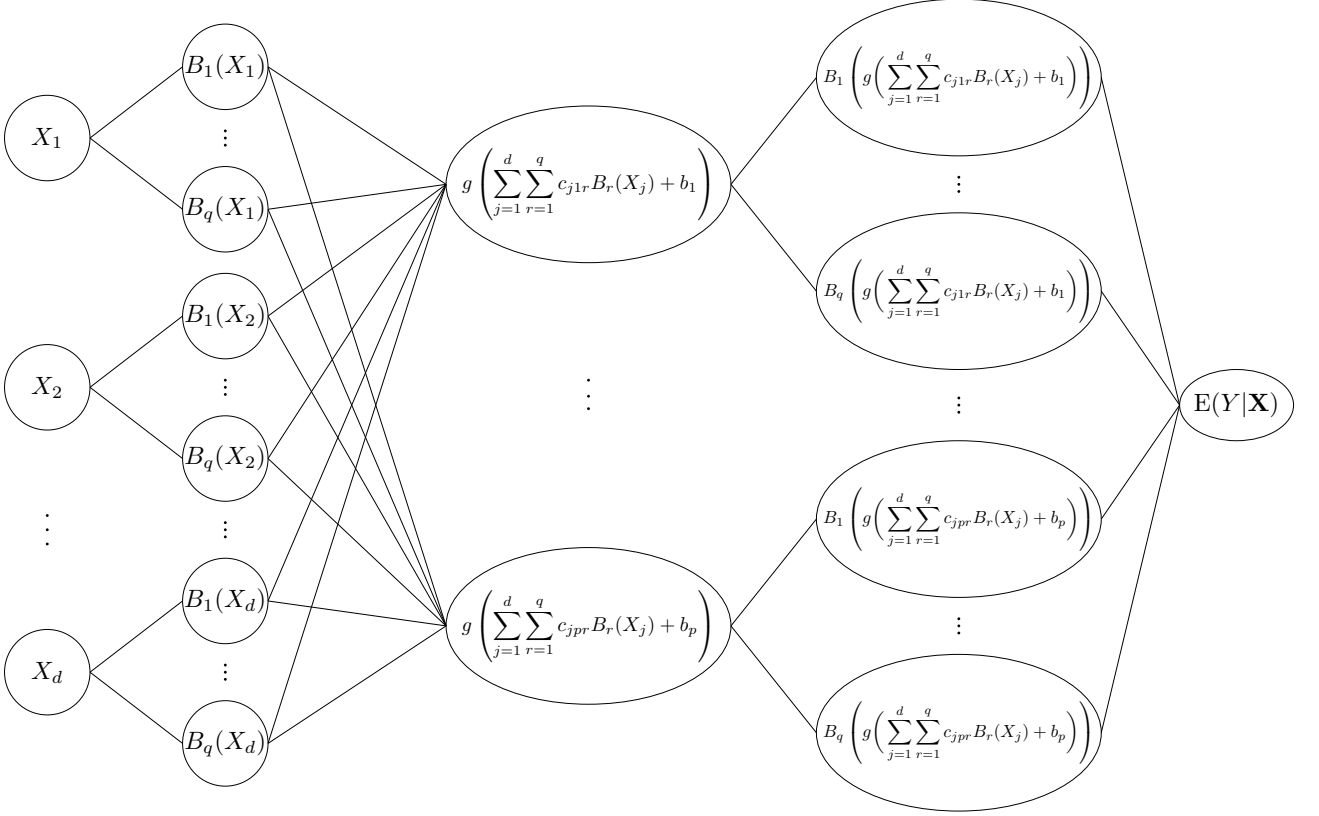


Figure 3: Architecture of ANN model in the case of the same set and same number of basis functions.

layers is illustrated in Figure 4. Formally, it can be written as

$$\begin{aligned}
 E(Y|\mathbf{X}) &= \sum_{k=1}^{p_L} \sum_{r=1}^{q_k} c_{kr} B_{kr}(X_k^{(L)}) + b, \\
 X_k^{(L)} &= g_L \left(\sum_{j=1}^{p_{L-1}} \sum_{r=1}^{q_{jk}^{(L)}} c_{jkr}^{(L)} B_{jkr}^{(L)}(X_j^{(L-1)}) + b_k^{(L)} \right) \text{ for } k = 1, \dots, p_L, \\
 &\vdots \\
 X_k^{(1)} &= g_1 \left(\sum_{j=1}^d \sum_{r=1}^{q_{jk}^{(1)}} c_{jkr}^{(1)} B_{jkr}^{(1)}(X_j) + b_k^{(1)} \right) \text{ for } k = 1, \dots, p_1,
 \end{aligned}
 \tag{2.4}$$

where p_l is the number of nodes in the l th hidden layer, $\{B_{kr} : r \geq 1\}$ and $\{B_{jkr}^{(l)} : r \geq 1\}$ are sets of basis functions, q_k and $q_{jk}^{(l)}$ are the numbers of used basis functions, $g_l : \mathbb{R} \rightarrow [0, 1]$ are functions, and $c_{kr}, c_{jkr}^{(l)}, b_k^{(l)}, b \in \mathbb{R}$ are parameters. We call (2.4) a Deep Additive Neural Network (DANN).

The advantages of ANN given in Remark 1 are still valid for the DANN. In particular, constructing basis functions in this network is easier than that in Liu et al. (2024) since the output values from g_l lie in $[0, 1]$, and hence we do not need to adapt basis functions in the next layer according to

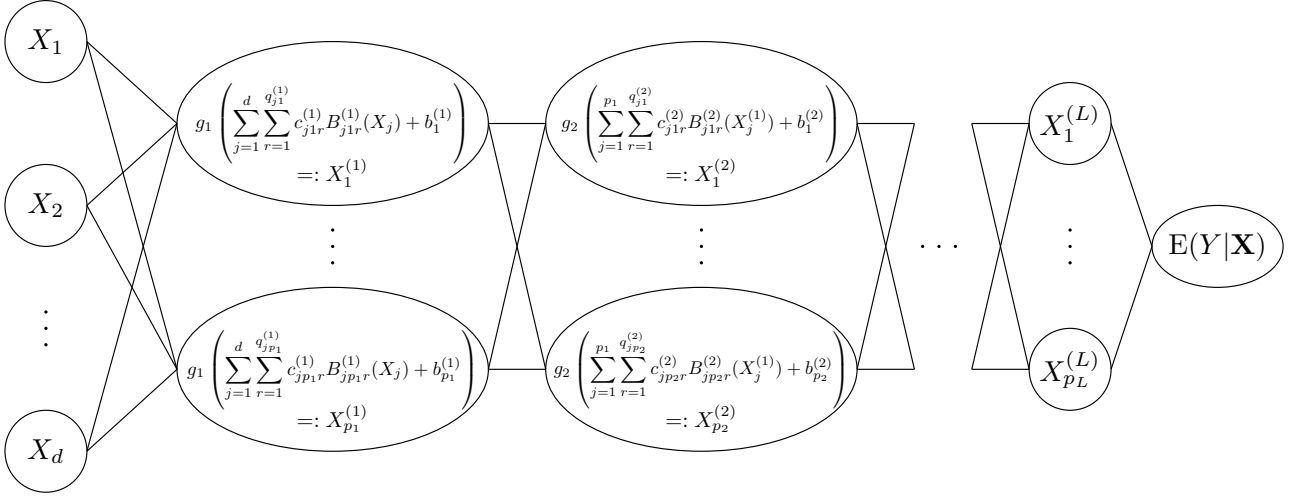


Figure 4: Architecture of DANN model.

the output values. In [Liu et al. \(2024\)](#), however, knots for the B-spline basis need to be adjusted according to the output values from their activation functions.

3 Hybrid Networks

The DANN may approximate a complex regression function well, but its complexity might be too high for a relatively simple regression function. In the latter case, it can overfit data. To adjust the model complexity, we introduce three networks that combine the architectures of ANN and DNN. These networks use the architecture of ANN for some layers and use that of DNN for other layers.

The first hybrid network, namely the Hybrid Deep Additive Neural Network 1 (HDANN1), uses the ANN architecture to construct the first hidden layer and uses the DNN architecture for the remaining layers. This network is illustrated in [Figure 5](#). Formally, it can be written as

$$\begin{aligned}
 \mathbb{E}(Y|\mathbf{X}) &= \sum_{k=1}^{p_L} w_k X_k^{(L)} + b, \\
 X_k^{(L)} &= \sigma_L \left(W_k^{(L)\top} \mathbf{X}^{(L-1)} + b_k^{(L)} \right) \text{ for } k = 1, \dots, p_L, \\
 &\vdots \\
 X_k^{(2)} &= \sigma_2 \left(W_k^{(2)\top} \mathbf{X}^{(1)} + b_k^{(2)} \right) \text{ for } k = 1, \dots, p_2, \\
 X_k^{(1)} &= \sigma_1 \left(\sum_{j=1}^d \sum_{r=1}^{q_{jk}} c_{jkr} B_{jkr}(X_j) + b_k^{(1)} \right) \text{ for } k = 1, \dots, p_1,
 \end{aligned}
 \tag{3.5}$$

where $W_k^{(l)} \in \mathbb{R}^{p_{l-1}}$ are vectors of weight parameters, $\mathbf{X}^{(l)} = (X_1^{(l)}, \dots, X_{p_l}^{(l)})^\top \in \mathbb{R}^{p_l}$, and $\sigma_l : \mathbb{R} \rightarrow \mathbb{R}$ are functions.

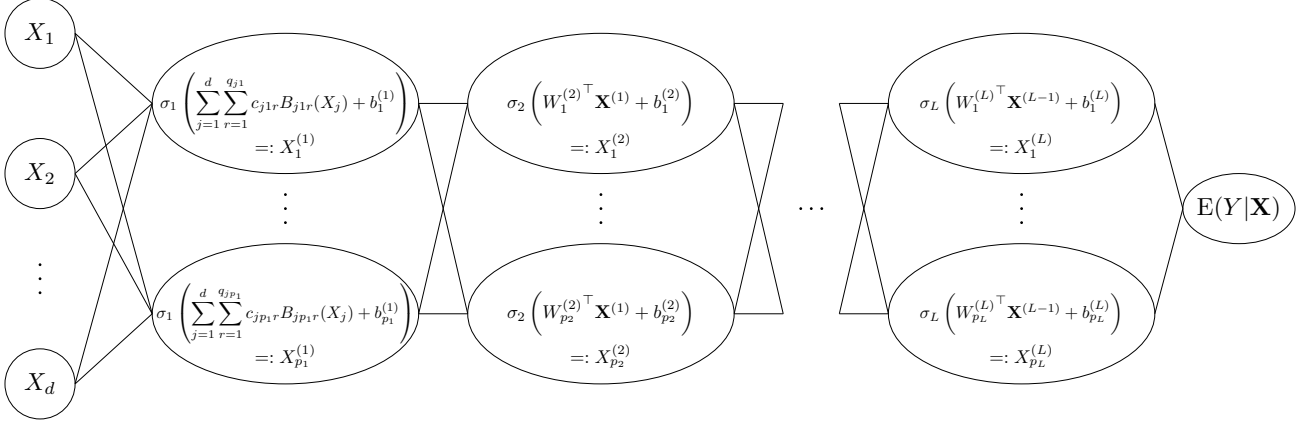


Figure 5: Architecture of HDANN1 model.

This network also has the universal approximation property even when $p_1 = \dots = p_L$ and $\sigma_1 = \dots = \sigma_L$. To describe this, let \mathbf{q} denote the collection of q_{jk} , \mathbf{W} denote the collection of $W_k^{(l)}$, \mathbf{c} denote the collection of c_{jkr} , and \mathbf{b} denote the collection of $b_k^{(l)}$ and b . Also, let

$$\text{HDANN1}_{L,\mathbf{q},\mathbf{W},\mathbf{c},\mathbf{b}}(\mathbf{x}) = \sum_{k=1}^{p_L} w_k x_k^{(L)} + b$$

denote the function on $[0, 1]^d$ defined through the architecture at (3.5).

Theorem 2. *Let $\{B_{jkr} : r \geq 1\}$ be any sets of basis functions, $p_1 = \dots = p_L \geq d + 3$, and $\sigma_1 = \dots = \sigma_L$ be a non-affine Lipschitz continuous function which is continuously differentiable at at least one point, with nonzero derivative at that point. Then, for any given continuous function $f : [0, 1]^d \rightarrow \mathbb{R}$ and constant $\epsilon > 0$, there exist $L, q_{jk} \geq 1$, $W_k^{(l)} \in \mathbb{R}^{p_{l-1}}$ and $c_{jkr}, b_k^{(l)}, b \in \mathbb{R}$ such that*

$$\sup_{\mathbf{x} \in [0, 1]^d} |f(\mathbf{x}) - \text{HDANN1}_{L,\mathbf{q},\mathbf{W},\mathbf{c},\mathbf{b}}(\mathbf{x})| < \epsilon.$$

Examples of σ_l satisfying the assumption in Theorem 2 include the logistic function, the rectified linear unit (ReLU) function and tanh.

The second hybrid network, namely the Hybrid Deep Additive Neural Network 2 (HDANN2), is the reverse version of HDANN1. It adopts the ANN architecture to construct the output layer and the DNN architecture for the hidden layers. This network is written below and visualized in Figure

6.

$$\begin{aligned}
\mathbb{E}(Y|\mathbf{X}) &= \sum_{k=1}^{p_L} \sum_{r=1}^{q_k} c_{kr} B_{kr}(X_k^{(L)}) + b, \\
X_k^{(L)} &= g_L \left(W_k^{(L)\top} \mathbf{X}^{(L-1)} + b_k^{(L)} \right) \text{ for } k = 1, \dots, p_L, \\
(3.6) \quad X_k^{(L-1)} &= \sigma_{L-1} \left(W_k^{(L-1)\top} \mathbf{X}^{(L-2)} + b_k^{(L-1)} \right) \text{ for } k = 1, \dots, p_{L-1}, \\
&\vdots \\
X_k^{(1)} &= \sigma_1 \left(W_k^{(1)\top} \mathbf{X} + b_k^{(1)} \right) \text{ for } k = 1, \dots, p_1,
\end{aligned}$$

where $g_L : \mathbb{R} \rightarrow [0, 1]$ and $\sigma_l : \mathbb{R} \rightarrow \mathbb{R}$ are functions.

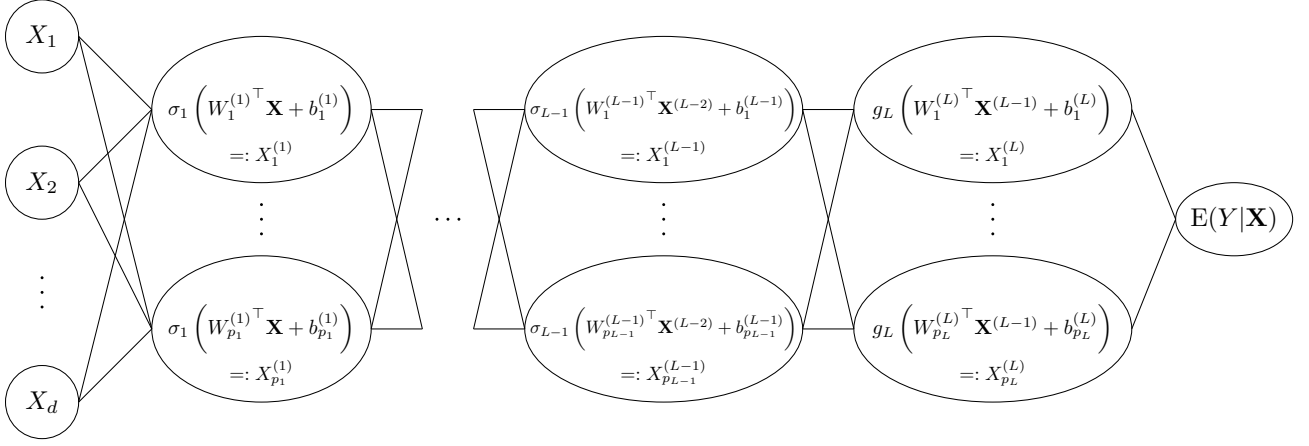


Figure 6: Architecture of HDANN2 model.

This network also has the universal approximation property even when $p_1 = \dots = p_L$ and $\sigma_1 = \dots = \sigma_{L-1} = g_L$. Define $\mathbf{q}, \mathbf{W}, \mathbf{c}$ and \mathbf{b} similarly as in the case of HDANN1 and let

$$\text{HDANN2}_{L,\mathbf{q},\mathbf{W},\mathbf{c},\mathbf{b}}(\mathbf{x}) = \sum_{k=1}^{p_L} \sum_{r=1}^{q_k} c_{kr} B_{kr}(x_k^{(L)}) + b$$

denote the function on $[0, 1]^d$ defined through the architecture at (3.6).

Theorem 3. *Let $\{B_{kr} : r \geq 1\}$ be any sets of basis functions, $p_1 = \dots = p_L \geq d + 3$, and $\sigma_1 = \dots = \sigma_{L-1} = g_L$ be a continuous function which is continuously differentiable at at least one point, with nonzero derivative at that point. Then, for any given continuous function $f : [0, 1]^d \rightarrow \mathbb{R}$ and constant $\epsilon > 0$, there exist $L, q_k \geq 1$, $W_k^{(l)} \in \mathbb{R}^{p_l-1}$ and $c_{kr}, b_k^{(l)}, b \in \mathbb{R}$ such that*

$$\sup_{\mathbf{x} \in [0, 1]^d} |f(\mathbf{x}) - \text{HDANN2}_{L,\mathbf{q},\mathbf{W},\mathbf{c},\mathbf{b}}(\mathbf{x})| < \epsilon.$$

The third hybrid network, namely the Hybrid Deep Additive Neural Network 3 (HDANN3), combines the HDANN1 and HDANN2. This network takes the ANN architecture for the first hidden layer and output layer and takes the DNN architecture for the remaining layers. This network is formulated below and depicted in Figure 7.

$$\begin{aligned}
E(Y|\mathbf{X}) &= \sum_{k=1}^{p_L} \sum_{r=1}^{q_k} c_{kr} B_{kr}(X_k^{(L)}) + b, \\
X_k^{(L)} &= g_L \left(W_k^{(L)\top} \mathbf{X}^{(L-1)} + b_k^{(L)} \right) \text{ for } k = 1, \dots, p_L, \\
X_k^{(L-1)} &= \sigma_{L-1} \left(W_k^{(L-1)\top} \mathbf{X}^{(L-2)} + b_k^{(L-1)} \right) \text{ for } k = 1, \dots, p_{L-1}, \\
&\vdots \\
X_k^{(2)} &= \sigma_2 \left(W_k^{(2)\top} \mathbf{X}^{(1)} + b_k^{(2)} \right) \text{ for } k = 1, \dots, p_2, \\
X_k^{(1)} &= \sigma_1 \left(\sum_{j=1}^d \sum_{r=1}^{q_{jk}} c_{jkr} B_{jkr}(X_j) + b_k^{(1)} \right) \text{ for } k = 1, \dots, p_1.
\end{aligned}
\tag{3.7}$$

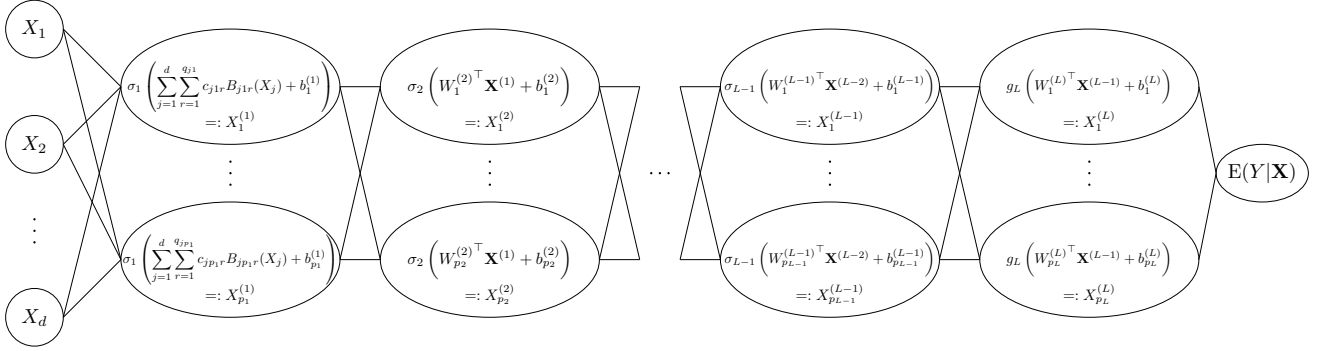


Figure 7: Architecture of HDANN3 model.

Note that the HDANN3 reduces to the ANN, which already has the universal approximation property, when there is a single hidden layer ($L = 1$).

4 Simulations

In this section, we compare the proposed networks (DANN, HDANN1, HDANN2 and HDANN3) with the DNN. We compare not only their prediction performance but also the numbers of parameters. We generated Y from the following two models:

$$\text{Model 1: } Y = \exp \left(\sum_{j=1}^3 X_j^3 - \sum_{j=4}^6 X_j^3 \right) + \varepsilon,
\tag{4.8}$$

$$\text{Model 2: } Y = (1 + X_1 + 2X_2^2 + 3X_3^3 - \exp(X_4) - \log(X_5 + 1) - |X_6 - 0.5|)^2 + \varepsilon,$$

where X_j were generated from the uniform distribution $U(0, 1)$ and the error term ε was generated from the normal distribution $N(0, 0.1^2)$ independently of \mathbf{X} .

To reduce the number of hyperparameter combinations, we used the same number of nodes and the same activation function across all hidden layers, that is, $p_l \stackrel{l}{\equiv} p$ and $\sigma_l \stackrel{l}{\equiv} \sigma$. For the DNN, we explored all combinations of $L \in \{2 \times t : 1 \leq t \leq 9\}$, $p \in \{2^t : t = 3, 5, 7, 9, 11\}$ and $\sigma \in \{\text{logistic}, \text{ReLU}, \text{tanh}\}$. This resulted in $9 \times 5 \times 3 = 135$ combinations for the DNN. For the proposed networks, we used the logistic function for all g_l . We also used the same set $\{B_r : r \geq 1\}$ of basis functions and the same number q of basis functions across all layers and nodes. We investigated all combinations of $L \in \{1, 3, 5, 7, 9\}$, $p \in \{2^t : t = 2, 4, 6, 8, 10\}$, $q \in \{3, 5, 7, 9, 11\}$ and $\sigma \in \{\text{logistic}, \text{ReLU}, \text{tanh}\}$, along with two basis options, $\{B_r(x) : r \geq 1\} = \{x^r : r \geq 1\}$ (polynomial) and $\{B_r(x) : r \geq 1\} = \{\cos(r\pi x) : r \geq 1\}$ (cosine). This resulted in $5 \times 5 \times 5 \times 3 \times 2 = 750$ combinations for each proposed network.

In this setting, the number of parameters for each network is given by

$$\begin{aligned}\#\text{DNN}(d, L, p) &= (d+1)p + (p+1)p(L-1) + p+1, \\ \#\text{DANN}(d, L, p, q) &= (dq+1)p + (pq+1)p(L-1) + pq+1, \\ \#\text{HDANN1}(d, L, p, q) &= (dq+1)p + (p+1)p(L-1) + p+1, \\ \#\text{HDANN2}(d, L, p, q) &= (d+1)p + (p+1)p(L-1) + pq+1, \\ \#\text{HDANN3}(d, L, p, q) &= (dq+1)p + (p+1)p(L-1) + pq+1.\end{aligned}$$

With the largest L, p and q for each network, it holds that

$$\begin{aligned}\#\text{DANN}(6, 9, 2^{10}, 11) &> \#\text{DNN}(6, 18, 2^{11}) \\ &> \#\text{HDANN3}(6, 9, 2^{10}, 11) > \#\text{HDANN1}(6, 9, 2^{10}, 11) > \#\text{HDANN2}(6, 9, 2^{10}, 11).\end{aligned}$$

For each model in (4.8), we generated 5 Monte-Carlo samples, with each sample consisting of a training set, a validation set and a test set. The sizes of the validation sets and test sets were fixed at 500, while the sizes of the training sets were either 1000 (scenario 1) or 2000 (scenario 2). In each training process, we used standardized response values Y_i^{st} . Here, the mean and standard deviation for the standardization were computed from the training set. The parameters were initialized using the Xavier uniform initialization (Glorot and Bengio (2010)) and then updated in the direction of minimizing $\sum_{i \in I_{\text{train}}} (Y_i^{\text{st}} - \hat{Y}_i^{\text{st}})^2$ using the ADAM optimization with a batch size of 512 and a learning rate of 10^{-4} , where I_{train} is the index set of the training set. To reduce computation time, we terminated the updating process if $\sum_{i \in I_{\text{train}}} (Y_i^{\text{st}} - \hat{Y}_i^{\text{st}})^2 / |I_{\text{train}}|$ does not decrease by more than 10^{-3} over the recent 10 updates, where $|I_{\text{train}}|$ denotes the cardinality of I_{train} .

After training the networks, we evaluated validation errors in the original response scale. Figure 8 displays the boxplots of $\sum_{i \in I_{\text{validation}}^{(1)}} (Y_i - \hat{Y}_i)^2 / 500$ across all hyperparameter combinations in the first Monte-Carlo sample, where $I_{\text{validation}}^{(1)}$ is the index set of the validation set in the first Monte-Carlo sample. We separated the boxplots for different basis types to see their effects. This figure shows that the DANN with cosine basis (DANN-C) generally yields higher validation errors compared to the DNN, while the other proposed networks tend to have lower validation errors than the DNN. This figure also reveals that the polynomial basis generally yields better performance than the cosine basis for the DANN and HDANN1, while the opposite trend holds for the HDANN2.

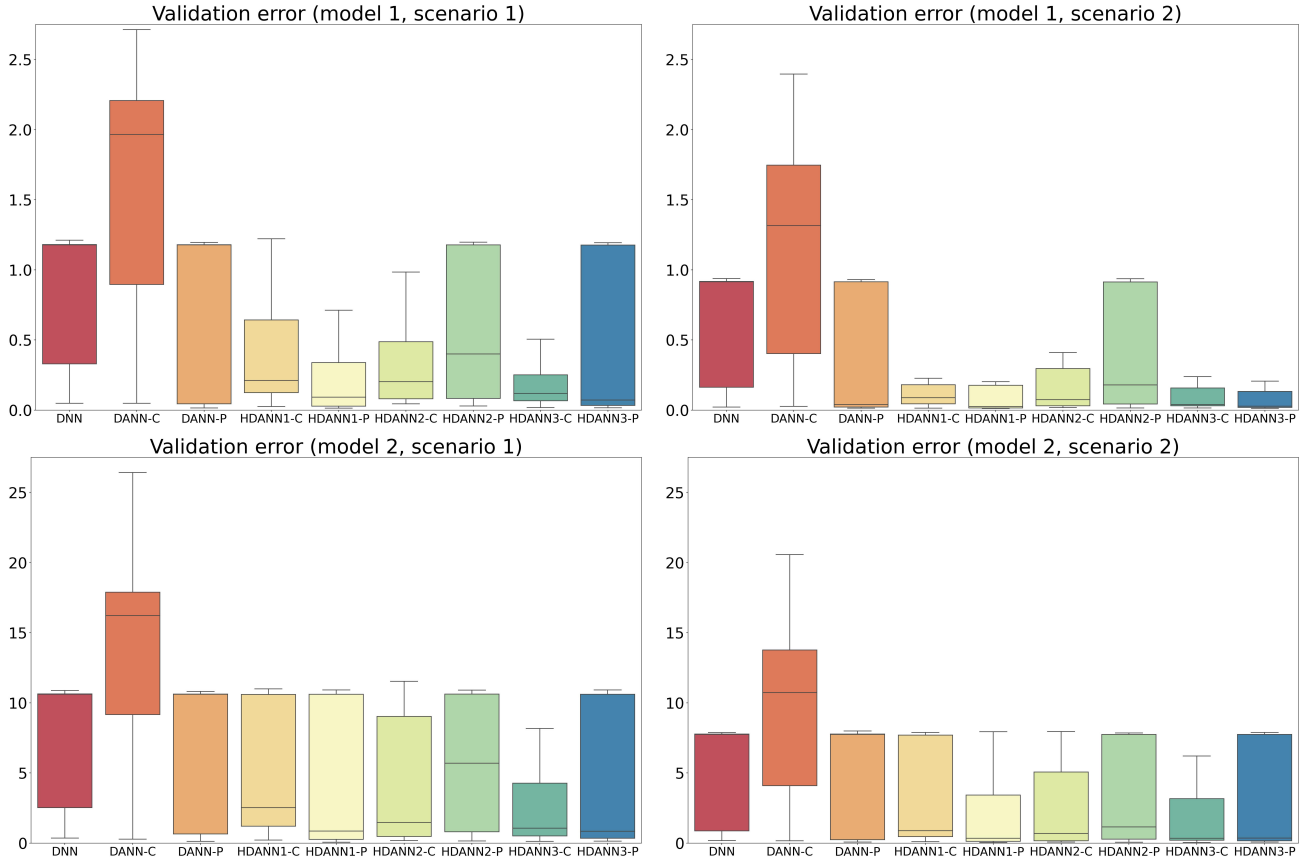


Figure 8: Boxplots of $\sum_{i \in I_{\text{validation}}^{(1)}} (Y_i - \hat{Y}_i)^2 / 500$. The median value and the Q3 value are almost overlapped for the DNN and the DANN with polynomial basis (DANN-P) in some scenarios.

Figure 9 illustrates the scatter plots of

$$\left(\log_{10}(\text{the number of parameters}), \sum_{i \in I_{\text{validation}}^{(1)}} (Y_i - \hat{Y}_i)^2 / 500 \right)$$

across hyperparameter combinations giving relatively low validation errors in the first Monte-Carlo sample. This figure shows that there always exist proposed networks that achieve lower validation

errors than the DNN with much fewer parameters. This demonstrates that adopting an additive layer can significantly reduce network sizes in deep learning.

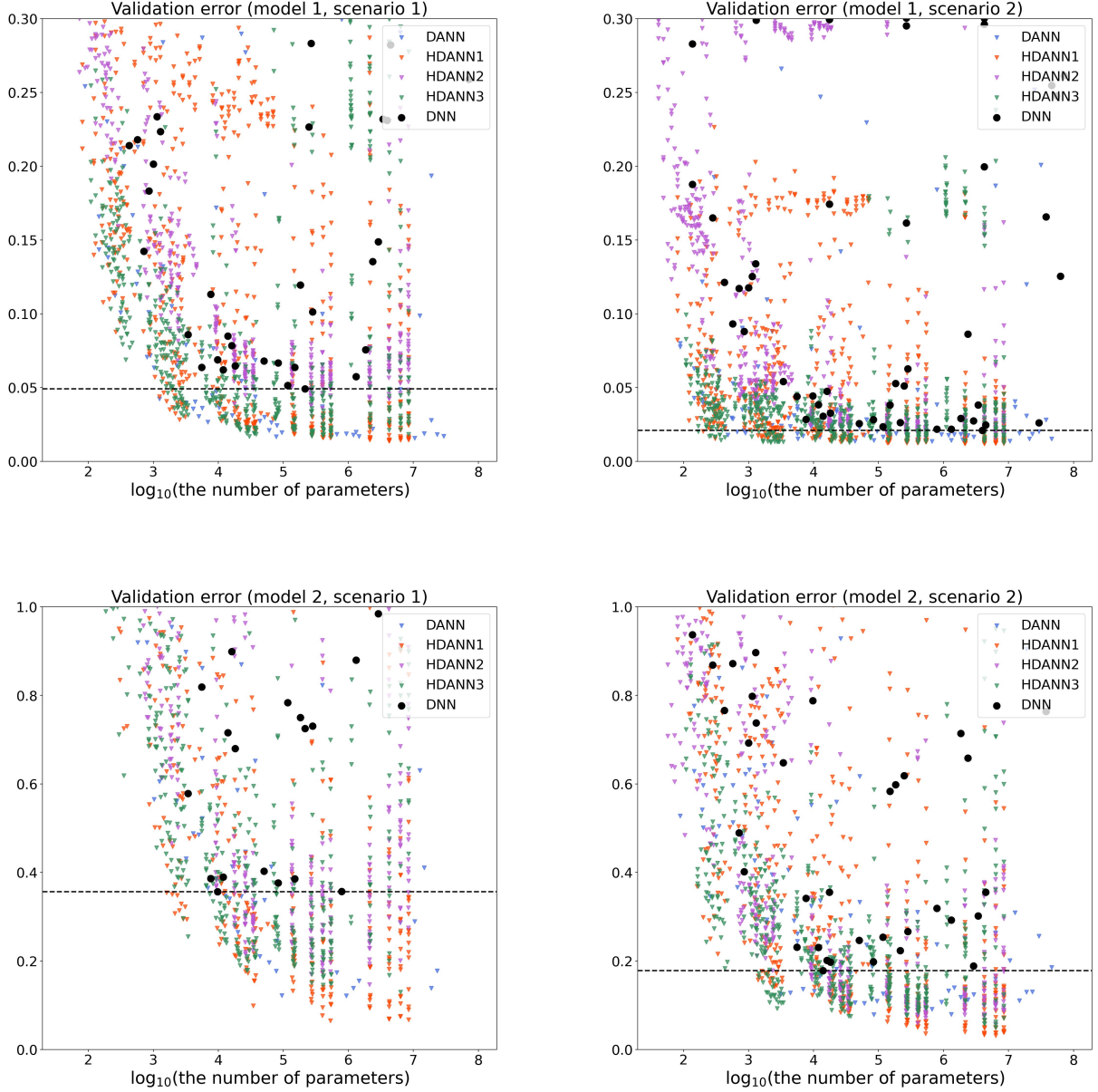


Figure 9: Scatter plots of $\log_{10}(\text{the number of parameters})$ versus $\sum_{i \in I_{\text{validation}}^{(1)}} (Y_i - \hat{Y}_i)^2 / 500$. The black dashed lines represent the smallest validation errors achieved by the DNN.

We also compared the average test errors defined by $5^{-1} \sum_{r=1}^5 \sum_{i \in I_{\text{test}}^{(r)}} (Y_i^{(r)} - \hat{Y}_i^{(r)})^2 / 500$, where $I_{\text{test}}^{(r)}$ is the index set of the test set in the r th Monte-Carlo sample, $Y_i^{(r)}$ are the response values in that test set and $\hat{Y}_i^{(r)}$ are their predicted values. In the comparison, we only selected either one or two hyperparameter combinations for each network and Monte-Carlo sample. For the DNN, we

chose the one giving the lowest validation error in each Monte-Carlo sample. For each proposed network, we chose not only the one giving the lowest validation error but also the one having the smallest number of parameters among hyperparameter combinations giving lower validation errors than the best-tuned DNN in each Monte-Carlo sample. The selected hyperparameter combinations are presented in Appendix 7.2. Table 1 shows that the best-tuned proposed networks significantly outperform the best-tuned DNN, with HDANN1 performing the best. Table 1 also shows that the error margins between them increase as the sample size increases. It also shows that the proposed networks equipped with small numbers of parameters have similar performance to the best-tuned DNN. In addition, Appendix 7.2 reveals that our networks have similar training times to the DNN. These results demonstrate that our networks are good alternatives to the DNN.

Table 1: Comparison of average test errors and average numbers of parameters (in parentheses). The networks hyphenated ‘best’ indicate the best-tuned networks and the networks hyphenated ‘small’ indicate those with the smallest numbers of parameters among hyperparameter combinations giving lower validation errors than the best-tuned DNN.

Network	Model 1		Model 2	
	Scenario 1	Scenario 2	Scenario 1	Scenario 2
DNN-best	0.03898 (169159.4)	0.02293 (901889.0)	0.31219 (32820.2)	0.05285 (168737.0)
DANN-best	0.01588 (8837837.8)	0.01466 (8847361.0)	0.11919 (816845.8)	0.02729 (4388353.0)
DANN-small	0.03298 (1876.2)	0.02006 (11602.6)	0.26156 (13106.6)	0.04165 (2107450.6)
HDANN1-best	0.01372 (4663297.0)	0.01202 (3813786.6)	0.05652 (5170586.6)	0.01601 (5498061.8)
HDANN1-small	0.03574 (1466.6)	0.02064 (4604.2)	0.27148 (1639.4)	0.04891 (8090.6)
HDANN2-best	0.02820 (1160909.8)	0.01664 (424858.6)	0.12950 (2610586.6)	0.02560 (2369434.6)
HDANN2-small	0.03460 (211809.0)	0.02192 (51137.0)	0.27421 (17505.0)	0.06055 (137897.0)
HDANN3-best	0.01688 (1576193.0)	0.01340 (6768385.0)	0.10530 (3053978.6)	0.02075 (3090330.6)
HDANN3-small	0.03544 (2273.0)	0.02147 (1223.4)	0.29031 (1889.0)	0.04992 (6636.2)

5 Real Data Analysis

We applied our methods to the California Housing data obtained from the *sklearn* Python library. This dataset consists of 9 variables across $n = 20640$ block groups. A block group is a geographical unit containing multiple houses. We took the logarithm of the median house value in each block group as Y and the following other variables as X_1, \dots, X_8 : *Longitude of block group*, *Latitude of block group*, *Median house age*, *Average number of rooms*, *Average number of bedrooms*, *Population*,

Average number of households and Median household income. With these notations, our dataset is written as $\{(X_{i1}, \dots, X_{i8}, Y_i) : 1 \leq i \leq n\}$.

To compare the networks, we randomly divided $\{1, \dots, n\}$ into 5 partitions, say $S^{(1)}, \dots, S^{(5)}$. We then computed the 5-fold average test errors defined by $5^{-1} \sum_{r=1}^5 \sum_{i \in S^{(r)}} (Y_i - \hat{Y}_i)^2 / |S^{(r)}|$, where \hat{Y}_i for $i \in S^{(r)}$ is the prediction of Y_i obtained without $\{Y_i : i \in S^{(r)}\}$. To obtain \hat{Y}_i for $i \in S^{(r)}$, we first divided $\{1, \dots, n\} \setminus S^{(r)}$ into a training set index ($S_{\text{train}}^{(r)}$) and a validation set index ($S_{\text{validation}}^{(r)}$) with the ratio 3 : 1 and scaled all X_{ij} by $(X_{ij} - X_{j,\min}^{(r)}) / (X_{j,\max}^{(r)} - X_{j,\min}^{(r)})$, where $X_{j,\min}^{(r)}$ and $X_{j,\max}^{(r)}$ are the minimum and maximum values of $\{X_{ij} : i \in S_{\text{train}}^{(r)}\}$, respectively. We then trained the networks using the standardized values of Y with mean and standard deviation being computed from $\{Y_i : i \in S_{\text{train}}^{(r)}\}$. Here, we took the same hyperparameter combinations and optimization as in the simulation study.

Figure 10 provides the boxplots of validation errors on $S_{\text{validation}}^{(1)}$ in the original response scale. It shows that the DANN is comparable with the DNN, while the hybrid networks tend to have significantly lower validation errors than the DNN. In particular, the cosine basis works better than the polynomial basis for the hybrid networks.

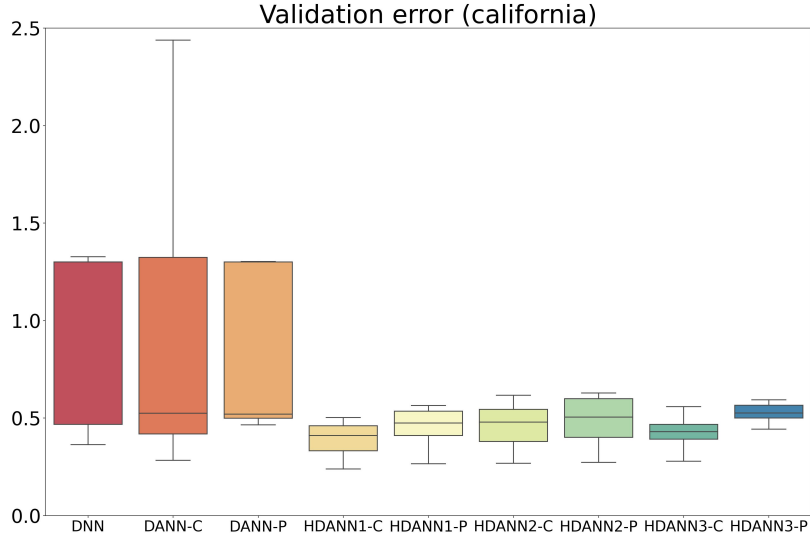


Figure 10: Boxplots of $\sum_{i \in S_{\text{validation}}^{(1)}} (Y_i - \hat{Y}_i)^2 / |S_{\text{validation}}^{(1)}|$. The DNN has almost the same median and Q3 values.

To compare the numbers of parameters, the scatter plot of

$$\left(\log_{10}(\text{the number of parameters}), \sum_{i \in S_{\text{validation}}^{(1)}} (Y_i - \hat{Y}_i)^2 / |S_{\text{validation}}^{(1)}| \right)$$

is drawn across hyperparameter combinations with relatively low validation errors (Figure 11). This figure illustrates that there are many proposed networks that have lower validation errors than the DNN. There also exist proposed networks that have approximately 10^4 -times fewer parameters but achieve lower validation errors than the DNN.

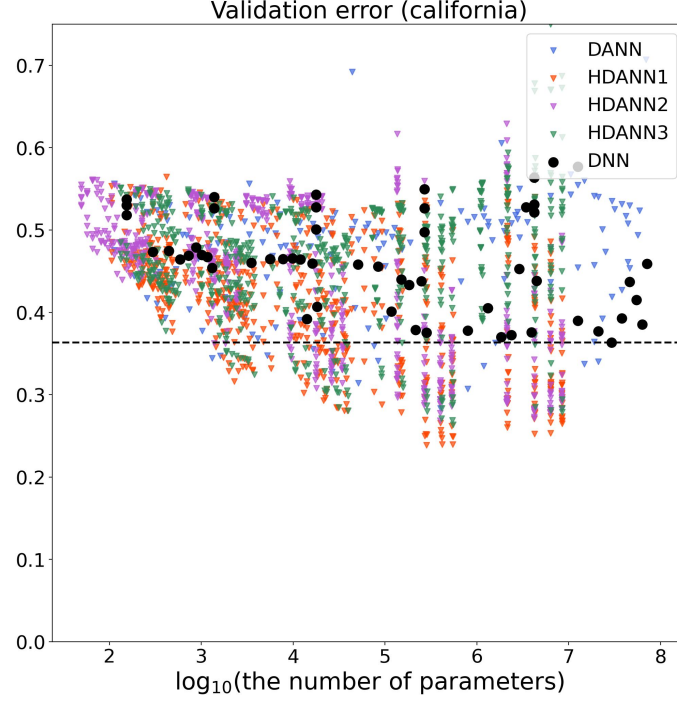


Figure 11: Scatter plot of $\log_{10}(\text{the number of parameters})$ versus $\sum_{i \in S_{\text{validation}}^{(1)}} (Y_i - \hat{Y}_i)^2 / |S_{\text{validation}}^{(1)}|$. The black dashed line represents the smallest validation error achieved by the DNN.

In the comparison of $5^{-1} \sum_{r=1}^5 \sum_{i \in S^{(r)}} (Y_i - \hat{Y}_i)^2 / |S^{(r)}|$, we only considered either one or two hyperparameter combinations for each network based on the errors on $S_{\text{validation}}^{(r)}$ similarly as in the simulation study. The selected hyperparameter combinations and the corresponding training times are provided in Appendix 7.3. Table 2 shows that all the best-tuned proposed networks significantly outperform the best-tuned DNN, with HDANN1 performing the best. In addition, the proposed networks equipped with small numbers of parameters have lower test errors than the best-tuned DNN. For example, HDANN1-small in Table 2 has nearly 10^4 -times fewer parameters than the best-tuned DNN in average. These results again confirm the superiority of our networks.

Table 2: Comparison of average test errors and average numbers of parameters (in parentheses) on the California Housing data.

Network	Test Error (# of Parameters)
DNN-best	0.38249 (8194458.6)
DANN-best	0.30345 (334823.4)
DANN-small	0.36606 (905.0)
HDANN1-best	0.24706 (332289.0)
HDANN1-small	0.37593 (794.6)
HDANN2-best	0.28298 (5549159.4)
HDANN2-small	0.36084 (5601.0)
HDANN3-best	0.27396 (493773.8)
HDANN3-small	0.37514 (1217.8)

6 Conclusion

In this works, we proposed a new nonlinear deep neural network along with hybrid variants. These networks are easy to implement due to the simple construction of activation and basis functions. Additionally, these networks achieve the universal approximation properties. We found that adding nonlinear layers enhances accuracy and can even reduce the number of parameters. The idea of this work can be applied to other topics, such as convolutional neural networks and classification problems, by making appropriate changes. We believe that our networks are promising alternatives to the traditional neural networks.

7 Appendix

7.1 Proofs

7.1.1 Proof of Lemma 1

The desired result holds for $B_r(x) = x^r$ since the space of all polynomials on $[0, 1]$ is a dense subset of the space of all continuous functions on $[0, 1]$ by the Weierstrass approximation theorem.

The desired result also holds for $B_r(x) = \cos(r\pi x)$. To see this, define a function $\Phi : [-\pi, \pi] \rightarrow \mathbb{R}$ by $\Phi(z) = \phi(z/\pi)\mathbf{I}(z \in [0, \pi]) + \phi(-z/\pi)\mathbf{I}(z \in [-\pi, 0])$. Then, Φ is an even continuous function, and

hence Fejér's theorem (e.g., Theorem 4.32 of [Pereyra and Ward \(2012\)](#)) implies that a function $\sigma_N \Phi$ defined by

$$\sigma_N \Phi(z) = \frac{1}{2\pi(N+1)} \sum_{k=0}^N \sum_{s=-k}^k \int_{-\pi}^{\pi} \Phi(t) (\cos(st) - \sqrt{-1} \sin(st)) dt (\cos(sz) + \sqrt{-1} \sin(sz))$$

converges uniformly to Φ . Since \sin is an odd function, we have $\int_{-\pi}^{\pi} \Phi(t) \sin(st) dt = 0$. This with the fact that Φ is real-valued implies that

$$\sigma_N \Phi(z) = \frac{1}{2\pi(N+1)} \sum_{k=0}^N \sum_{s=-k}^k \int_{-\pi}^{\pi} \Phi(t) \cos(st) dt \cos(sz)$$

converges uniformly to Φ . Note that $\sigma_N \Phi(z)$ is a linear combination of $\{\cos(sx) : 0 \leq s \leq N\}$ since \cos is an even function. Hence, for given $\epsilon > 0$, there exists $N \geq 0$ and $c_s \in \mathbb{R}$ such that $\sup_{z \in [0, \pi]} |\Phi(z) - \sum_{s=0}^N c_s \cos(sz)| < \epsilon$. This implies that $\sup_{x \in [0, 1]} |\phi(x) - \sum_{s=0}^N c_s \cos(s\pi x)| < \epsilon$.

Lastly, it is well known that the desired result holds for the Haar basis on $[0, 1]$; see [McLaughlin \(1969\)](#), for example. \square

7.1.2 Proof of Theorem 1

The universal approximation theorem ([Cybenko \(1989\)](#)) implies that there exist constants $p \geq 1$ and $w_k, w_{jk}, a_k \in \mathbb{R}$ such that

$$\sup_{\mathbf{x} \in [0, 1]^d} \left| f(\mathbf{x}) - \left(\sum_{k=1}^p w_k g \left(\sum_{j=1}^d w_{jk} x_j + a_k \right) \right) \right| < \frac{\epsilon}{2}.$$

Note that the functions $h_k : x \mapsto w_k x$ and $h_{jk} : x_j \mapsto w_{jk} x_j + a_k/d$ are uniformly continuous on $[0, 1]$. Hence, there exists $\delta_k > 0$ such that

$$\sup_{x, y \in [0, 1] : |x - y| < \delta_k} |h_k(x) - h_k(y)| < \frac{\epsilon}{4p}.$$

By the definitions of B_{jkr} and $B_{k\ell}$, there exist constants $q_k, q_{jk} \geq 1$ and $c_{k\ell}, b_k, c_{jkr}, b_{jk} \in \mathbb{R}$ such that

$$\begin{aligned} \sup_{x \in [0, 1]} \left| h_k(x) - \left(\sum_{\ell=1}^{q_k} c_{k\ell} B_{k\ell}(x) + b_k \right) \right| &< \frac{\epsilon}{4p}, \\ \sup_{x_j \in [0, 1]} \left| h_{jk}(x_j) - \left(\sum_{r=1}^{q_{jk}} c_{jkr} B_{jkr}(x_j) + b_{jk} \right) \right| &< \frac{\delta_k}{dL}, \end{aligned}$$

where $L > 0$ is the Lipschitz constant of g . Define

$$\tilde{h}_k(x) = \sum_{\ell=1}^{q_k} c_{k\ell} B_{k\ell}(x) + b_k,$$

$$\tilde{h}_{jk}(x_j) = \sum_{r=1}^{q_{jk}} c_{jkr} B_{jkr}(x_j) + b_{jk}.$$

Note that

$$\begin{aligned} \left| g \left(\sum_{j=1}^d h_{jk}(x_j) \right) - g \left(\sum_{j=1}^d \tilde{h}_{jk}(x_j) \right) \right| &\leq L \left| \sum_{j=1}^d h_{jk}(x_j) - \sum_{j=1}^d \tilde{h}_{jk}(x_j) \right| \\ &\leq L \sum_{j=1}^d |h_{jk}(x_j) - \tilde{h}_{jk}(x_j)| \\ &\leq \delta_k. \end{aligned}$$

Then,

$$\begin{aligned} &\sup_{\mathbf{x} \in [0,1]^d} \left| \sum_{k=1}^p h_k \left(g \left(\sum_{j=1}^d h_{jk}(x_j) \right) \right) - \sum_{k=1}^p \tilde{h}_k \left(g \left(\sum_{j=1}^d \tilde{h}_{jk}(x_j) \right) \right) \right| \\ &\leq \sup_{\mathbf{x} \in [0,1]^d} \sum_{k=1}^p \left| h_k \left(g \left(\sum_{j=1}^d h_{jk}(x_j) \right) \right) - \tilde{h}_k \left(g \left(\sum_{j=1}^d \tilde{h}_{jk}(x_j) \right) \right) \right| \\ &\leq \sup_{\mathbf{x} \in [0,1]^d} \sum_{k=1}^p \left| h_k \left(g \left(\sum_{j=1}^d h_{jk}(x_j) \right) \right) - h_k \left(g \left(\sum_{j=1}^d \tilde{h}_{jk}(x_j) \right) \right) \right| \\ &\quad + \sup_{\mathbf{x} \in [0,1]^d} \sum_{k=1}^p \left| h_k \left(g \left(\sum_{j=1}^d \tilde{h}_{jk}(x_j) \right) \right) - \tilde{h}_k \left(g \left(\sum_{j=1}^d \tilde{h}_{jk}(x_j) \right) \right) \right| \\ &\leq \sum_{k=1}^p \sup_{\mathbf{x} \in [0,1]^d} \left| h_k \left(g \left(\sum_{j=1}^d h_{jk}(x_j) \right) \right) - h_k \left(g \left(\sum_{j=1}^d \tilde{h}_{jk}(x_j) \right) \right) \right| \\ &\quad + \sum_{k=1}^p \sup_{\mathbf{x} \in [0,1]^d} \left| h_k \left(g \left(\sum_{j=1}^d \tilde{h}_{jk}(x_j) \right) \right) - \tilde{h}_k \left(g \left(\sum_{j=1}^d \tilde{h}_{jk}(x_j) \right) \right) \right| \\ &\leq \sum_{k=1}^p \sup_{x,y \in [0,1]: |x-y| < \delta_k} |h_k(x) - h_k(y)| + \sum_{k=1}^p \sup_{x \in [0,1]} |h_k(x) - \tilde{h}_k(x)| \\ &\leq \frac{\epsilon}{4} + \frac{\epsilon}{4}. \end{aligned}$$

Therefore,

$$\begin{aligned} &\sup_{\mathbf{x} \in [0,1]^d} \left| f(\mathbf{x}) - \sum_{k=1}^p \tilde{h}_k \left(g \left(\sum_{j=1}^d \tilde{h}_{jk}(x_j) \right) \right) \right| \\ &\leq \sup_{\mathbf{x} \in [0,1]^d} \left| f(\mathbf{x}) - \sum_{k=1}^p h_k \left(g \left(\sum_{j=1}^d h_{jk}(x_j) \right) \right) \right| \\ &\quad + \sup_{\mathbf{x} \in [0,1]^d} \left| \sum_{k=1}^p h_k \left(g \left(\sum_{j=1}^d h_{jk}(x_j) \right) \right) - \sum_{k=1}^p \tilde{h}_k \left(g \left(\sum_{j=1}^d \tilde{h}_{jk}(x_j) \right) \right) \right| \\ &< \epsilon. \end{aligned}$$

7.1.3 Proof of Theorem 2

Write $\sigma_1 = \dots = \sigma_L = \sigma$. By Theorem 3.2 of [Kidger and Lyons \(2020\)](#), there exist $L \geq 1$, $W_k^{(1)} \in \mathbb{R}^d$, $W_k^{(2)}, \dots, W_k^{(L)} \in \mathbb{R}^{d+3}$ and $w_k, a_k^{(1)}, b_k^{(l)}, b \in \mathbb{R}$ such that

$$\sup_{\mathbf{x} \in [0,1]^d} \left| f(\mathbf{x}) - \left(\sum_{k=1}^{d+3} w_k \tilde{x}_k^{(L)} + b \right) \right| < \frac{\epsilon}{2},$$

where

$$\tilde{x}_k^{(l)} = \sigma \left(W_k^{(l)\top} \tilde{\mathbf{x}}^{(l-1)} + b_k^{(l)} \right)$$

for $1 \leq k \leq d+3$ and $2 \leq l \leq L$, and

$$\tilde{x}_k^{(1)} = \sigma \left(W_k^{(1)\top} \mathbf{x} + a_k^{(1)} \right)$$

for $1 \leq k \leq d+3$. Define $M = \max\{|w_1|, \dots, |w_{d+3}|\}$ and $M_{kl} = \|W_k^{(l)}\|_\infty$. Let $C > 0$ denote the Lipschitz constant of σ . Define $h_{jk} : [0,1] \rightarrow \mathbb{R}$ by $h_{jk}(x_j) = W_{kj}^{(1)} x_j + a_k^{(1)}/d$, where $W_{kj}^{(1)}$ is the j th entry of $W_k^{(1)}$. Then, h_{jk} is a continuous function on $[0,1]$. By Lemma 1, there exist constants $q_{jk} \geq 1$ and $c_{jkr}, b_{jk} \in \mathbb{R}$ such that

$$\sup_{x_j \in [0,1]} \left| h_{jk}(x_j) - \left(\sum_{r=1}^{q_{jk}} c_{jkr} B_{jkr}(x_j) + b_{jk} \right) \right| < \frac{\epsilon}{2MC^L (\max_{1 \leq k \leq d+3, 2 \leq l \leq L} M_{kl}) (d+3)^L d}.$$

Define $\bar{h}_{jk}(x_j) = \sum_{r=1}^{q_{jk}} c_{jkr} B_{jkr}(x_j) + b_{jk}$. Then,

$$\begin{aligned} & \sup_{\mathbf{x} \in [0,1]^d} \left| \sigma \left(W_k^{(1)\top} \mathbf{x} + a_k^{(1)} \right) - \sigma \left(\sum_{j=1}^d \bar{h}_{jk}(x_j) \right) \right| \\ & \leq C \sup_{\mathbf{x} \in [0,1]^d} \left| \sum_{j=1}^d h_{jk}(x_j) - \sum_{j=1}^d \bar{h}_{jk}(x_j) \right| \\ & \leq C \sup_{\mathbf{x} \in [0,1]^d} \sum_{j=1}^d |h_{jk}(x_j) - \bar{h}_{jk}(x_j)| \\ & \leq \frac{\epsilon}{2MC^{L-1} (\max_{1 \leq k \leq d+3, 2 \leq l \leq L} M_{kl}) (d+3)^L} \end{aligned}$$

Define

$$x_k^{(l)} = \sigma \left(W_k^{(l)\top} \mathbf{x}^{(l-1)} + b_k^{(l)} \right)$$

for $1 \leq k \leq d+3$ and $2 \leq l \leq L$, and

$$x_k^{(1)} = \sigma \left(\sum_{j=1}^d \bar{h}_{jk}(x_j) \right).$$

Since

$$\begin{aligned} \left| \sigma \left(W_k^{(l)\top} \tilde{\mathbf{x}}^{(l-1)} + b_k^{(l)} \right) - \sigma \left(W_k^{(l)\top} \mathbf{x}^{(l-1)} + b_k^{(l)} \right) \right| &\leq C |W_k^{(l)\top} (\tilde{\mathbf{x}}^{(l-1)} - \mathbf{x}^{(l-1)})| \\ &\leq C M_{kl} \sum_{s=1}^{d+3} |\tilde{x}_s^{(l-1)} - x_s^{(l-1)}| \end{aligned}$$

for $2 \leq l \leq L$, we get

$$\begin{aligned} &\sup_{\mathbf{x} \in [0,1]^d} \left| \sum_{k=1}^{d+3} w_k \tilde{x}_k^{(L)} + b - \left(\sum_{k=1}^{d+3} w_k x_k^{(L)} + b \right) \right| \\ &\leq \sup_{\mathbf{x} \in [0,1]^d} M \sum_{k=1}^{d+3} |\tilde{x}_k^{(L)} - x_k^{(L)}| \\ &\leq \sup_{\mathbf{x} \in [0,1]^d} MC \sum_{k=1}^{d+3} M_{kL} \sum_{s=1}^{d+3} |\tilde{x}_s^{(L-1)} - x_s^{(L-1)}| \\ &\leq \dots \\ &\leq \sup_{\mathbf{x} \in [0,1]^d} MC^{L-1} \left(\max_{1 \leq k \leq d+3, 2 \leq l \leq L} M_{kl} \right) (d+3)^{L-1} \sum_{s=1}^{d+3} |\tilde{x}_s^{(1)} - x_s^{(1)}| \\ &\leq \frac{\epsilon}{2}. \end{aligned}$$

Therefore,

$$\sup_{\mathbf{x} \in [0,1]^d} \left| f(\mathbf{x}) - \left(\sum_{k=1}^{d+3} w_k x_k^{(L)} + b \right) \right| < \epsilon.$$

7.1.4 Proof of Theorem 3

Write $\sigma_1 = \dots = \sigma_{L-1} = g_L = \sigma$. By Theorem 3.2 of [Kidger and Lyons \(2020\)](#), there exist $L \geq 1$, $W_k^{(1)} \in \mathbb{R}^d$, $W_k^{(2)}, \dots, W_k^{(L)} \in \mathbb{R}^{d+3}$ and $w_k, b_k^{(l)}, a \in \mathbb{R}$ such that

$$\sup_{\mathbf{x} \in [0,1]^d} \left| f(\mathbf{x}) - \left(\sum_{k=1}^{d+3} w_k x_k^{(L)} + a \right) \right| < \frac{\epsilon}{2},$$

where

$$x_k^{(l)} = \sigma \left(W_k^{(l)\top} \mathbf{x}^{(l-1)} + b_k^{(l)} \right)$$

for $1 \leq k \leq d+3$ and $2 \leq l \leq L$, and

$$x_k^{(1)} = \sigma \left(W_k^{(1)\top} \mathbf{x} + b_k^{(1)} \right)$$

for $1 \leq k \leq d+3$. Define $h_k : [0, 1] \rightarrow \mathbb{R}$ by $h_k(x_k) = w_k x_k + a/(d+3)$. Then, h_k is a continuous function on $[0, 1]$. By Lemma 1, there exist constants $q_k \geq 1$ and $c_{kr}, b_k \in \mathbb{R}$ such that

$$\sup_{x_k \in [0, 1]} \left| h_k(x_k) - \left(\sum_{r=1}^{q_k} c_{kr} B_{kr}(x_k) + b_k \right) \right| < \frac{\epsilon}{2(d+3)}.$$

Then,

$$\sup_{\mathbf{x} \in [0, 1]^d} \left| \sum_{k=1}^{d+3} h_k(x_k) - \sum_{k=1}^{d+3} \left(\sum_{r=1}^{q_k} c_{kr} B_{kr}(x_k) + b_k \right) \right| < \frac{\epsilon}{2}.$$

Therefore,

$$\sup_{\mathbf{x} \in [0, 1]^d} \left| f(\mathbf{x}) - \sum_{k=1}^{d+3} \left(\sum_{r=1}^{q_k} c_{kr} B_{kr}(x_k^{(L)}) + b_k \right) \right| < \epsilon.$$

7.2 Selected hyperparameters for Table 1

Table 3: Model 1 in scenario 1

Monte-Carlo sample	Network	L	p	q	σ	B_r	Validation Error	Test Error	Training Time (sec)	# of Parameters
1st	DNN-best	14	128		tanh		0.04912	0.03219	10.13	215681
	DANN-best	3	1024	5		poly	0.01568	0.01699	10.40	10524673
	DANN-small	1	16	11		poly	0.04245	0.04857	10.29	1249
	HDANN1-best	5	1024	7	ReLU	poly	0.01375	0.01594	3.84	4243457
	HDANN1-small	3	16	7	ReLU	poly	0.04384	0.04862	9.26	1249
	HDANN2-best	7	256	9	tanh	poly	0.02946	0.01961	13.14	398849
	HDANN2-small	5	64	9	tanh	poly	0.03890	0.02693	16.46	17665
	HDANN3-best	9	256	11	ReLU	poly	0.01648	0.01751	9.65	546305
	HDANN3-small	5	16	5	ReLU	poly	0.04639	0.04658	12.87	1665
2nd	DNN-best	16	128		tanh		0.03601	0.04036	16.61	248705
	DANN-best	3	256	5		poly	0.01563	0.01482	9.82	665089
	DANN-small	9	4	11		poly	0.02473	0.02340	110.74	1753
	HDANN1-best	7	1024	5	ReLU	poly	0.01280	0.01269	5.67	6330369
	HDANN1-small	3	16	5	ReLU	poly	0.03287	0.03253	13.12	1057
	HDANN2-best	9	256	5	tanh	poly	0.02912	0.02662	17.63	529409
	HDANN2-small	9	256	5	tanh	poly	0.02912	0.02662	17.63	529409
	HDANN3-best	9	256	5	ReLU	poly	0.01526	0.01437	8.36	535553
	HDANN3-small	5	4	7	ReLU	poly	0.02893	0.03243	44.98	281
3th	DNN-best	12	128		tanh		0.03655	0.03968	13.85	182657
	DANN-best	3	256	11		poly	0.01530	0.01723	13.32	1462273
	DANN-small	1	16	11		poly	0.03546	0.04420	17.96	1249
	HDANN1-best	5	1024	9	ReLU	poly	0.01419	0.01524	5.36	4255745
	HDANN1-small	3	16	7	ReLU	poly	0.03300	0.03943	10.67	1249
	HDANN2-best	7	256	5	tanh	poly	0.02505	0.02811	15.29	397825
	HDANN2-small	9	64	3	tanh	cos	0.03651	0.03975	15.10	33921
	HDANN3-best	7	256	11	ReLU	poly	0.01555	0.01936	10.87	414721
	HDANN3-small	5	16	5	ReLU	poly	0.03628	0.04354	17.56	1665
4th	DNN-best	12	128		tanh		0.04206	0.03322	17.76	182657
	DANN-best	5	1024	5		poly	0.01798	0.01697	21.24	21012481
	DANN-small	1	64	9		poly	0.03951	0.04386	17.93	4097
	HDANN1-best	7	1024	7	ReLU	poly	0.01461	0.01387	6.80	6342657
	HDANN1-small	5	16	9	ReLU	poly	0.03809	0.03149	13.40	1985
	HDANN2-best	5	256	11	tanh	poly	0.03115	0.02291	18.35	267777
	HDANN2-small	5	256	5	tanh	poly	0.03815	0.02401	18.90	266241
	HDANN3-best	7	1024	7	ReLU	poly	0.02388	0.02013	10.95	6348801
	HDANN3-small	1	64	7	sigmoid	poly	0.04018	0.03666	18.00	7361
5th	DNN-best	16	32		tanh		0.03117	0.04580	21.02	16097
	DANN-best	3	1024	5		poly	0.01481	0.02156	13.26	10524673
	DANN-small	5	4	11		poly	0.02274	0.06149	58.08	1033
	HDANN1-best	3	1024	7	ReLU	poly	0.01323	0.01779	3.87	2144257
	HDANN1-small	5	16	7	ReLU	poly	0.03088	0.05785	12.18	1793
	HDANN2-best	5	1024	5	ReLU	poly	0.02621	0.03963	9.37	4210689
	HDANN2-small	7	64	3	tanh	poly	0.03031	0.03333	19.76	25601
	HDANN3-best	9	64	5	ReLU	poly	0.01324	0.03074	11.70	35585
	HDANN3-small	5	4	11	ReLU	poly	0.02543	0.08000	40.19	393

Table 4: Model 1 in scenario 2

Monte-Carlo sample	Network	L	p	q	σ	B_r	Validation Error	Test Error	Training Time (sec)	# of Parameters
1st	DNN-best	16	512		tanh		0.02109	0.02620	12.09	3943937
	DANN-best	3	256	5		poly	0.01359	0.01867	8.99	665089
	DANN-small	5	4	5		poly	0.01780	0.07074	56.97	481
	HDANN1-best	3	1024	7	ReLU	poly	0.01202	0.01208	2.94	2144257
	HDANN1-small	7	4	3	tanh	poly	0.02038	0.07681	28.59	201
	HDANN2-best	7	256	11	tanh	poly	0.01467	0.01718	12.48	399361
	HDANN2-small	9	64	3	tanh	cos	0.02015	0.02593	11.05	33921
	HDANN3-best	9	1024	5	ReLU	poly	0.01250	0.01468	8.10	8433665
	HDANN3-small	5	4	3	ReLU	poly	0.02018	0.07378	36.35	169
2nd	DNN-best	14	128		tanh		0.02070	0.02301	17.24	215681
	DANN-best	5	64	5		poly	0.01538	0.01819	16.72	84481
	DANN-small	3	64	5		poly	0.01813	0.02135	13.46	43393
	HDANN1-best	3	1024	3	ReLU	poly	0.01241	0.01321	4.77	2119681
	HDANN1-small	3	64	3	ReLU	poly	0.01833	0.02230	10.34	9601
	HDANN2-best	7	256	3	tanh	poly	0.01590	0.01649	18.45	397313
	HDANN2-small	3	256	9	ReLU	poly	0.02059	0.02855	12.28	135681
	HDANN3-best	9	1024	11	ReLU	cos	0.01355	0.01352	25.08	8476673
	HDANN3-small	5	16	7	ReLU	poly	0.01978	0.02478	20.49	1889
3rd	DNN-best	10	128		tanh		0.02610	0.02591	15.79	149633
	DANN-best	5	1024	5		poly	0.01456	0.01319	17.99	21012481
	DANN-small	5	4	7		poly	0.02309	0.01890	74.93	665
	HDANN1-best	7	1024	7	ReLU	poly	0.01187	0.01130	7.75	6342657
	HDANN1-small	3	16	7	ReLU	poly	0.02364	0.02176	12.15	1249
	HDANN2-best	9	256	11	tanh	poly	0.01865	0.01667	16.91	530945
	HDANN2-small	5	64	9	tanh	poly	0.02434	0.02193	23.82	17665
	HDANN3-best	9	1024	5	tanh	poly	0.01469	0.01302	11.89	8433665
	HDANN3-small	3	16	7	tanh	poly	0.02538	0.02414	16.85	1345
4th	DNN-best	6	128		tanh		0.02436	0.02902	18.31	83585
	DANN-best	3	256	11		poly	0.01415	0.01701	17.04	1462273
	DANN-small	3	16	5		poly	0.02229	0.03963	21.83	3169
	HDANN1-best	5	1024	5	ReLU	poly	0.01086	0.01405	6.45	4231169
	HDANN1-small	5	16	5	ReLU	poly	0.02143	0.02873	16.33	1601
	HDANN2-best	7	256	3	tanh	poly	0.01710	0.02494	18.03	397313
	HDANN2-small	5	64	3	tanh	poly	0.02356	0.03438	37.03	17281
	HDANN3-best	9	64	5	ReLU	poly	0.01241	0.02034	14.32	35585
	HDANN3-small	7	4	9	ReLU	poly	0.01990	0.03804	48.33	377
5th	DNN-best	8	128		tanh		0.02241	0.02759	19.14	116609
	DANN-best	5	1024	5		poly	0.01560	0.01401	13.94	21012481
	DANN-small	5	16	9		poly	0.01897	0.02040	21.15	10305
	HDANN1-best	5	1024	5	ReLU	poly	0.01295	0.01246	3.77	4231169
	HDANN1-small	3	64	5	ReLU	poly	0.01943	0.01983	6.70	10369
	HDANN2-best	7	256	11	tanh	poly	0.01688	0.02023	15.58	399361
	HDANN2-small	7	64	3	tanh	poly	0.02094	0.02423	24.07	25601
	HDANN3-best	9	1024	9	ReLU	cos	0.01385	0.01434	11.32	8462337
	HDANN3-small	5	16	11	tanh	poly	0.02213	0.01978	18.55	2337

Table 5: Model 2 in scenario 1

Monte-Carlo sample	Network	L	p	q	σ	B_r	Validation Error	Test Error	Training Time (sec)	# of Parameters
1st	DNN-best	10	32		tanh		0.35643	0.26051	13.14	9761
	DANN-best	3	256	7		poly	0.12137	0.09770	7.58	930817
	DANN-small	1	256	7		poly	0.34713	0.35049	10.34	12801
	HDANN1-best	9	256	3	ReLU	poly	0.06505	0.07388	5.51	531457
	HDANN1-small	5	16	5	ReLU	poly	0.35420	0.24014	9.36	1601
	HDANN2-best	3	1024	9	tanh	poly	0.14653	0.12778	10.39	2115585
	HDANN2-small	5	64	5	tanh	cos	0.29902	0.18741	10.02	17409
	HDANN3-best	7	1024	7	tanh	cos	0.12975	0.09299	10.43	6348801
	HDANN3-small	7	16	11	ReLU	poly	0.29647	0.27922	18.93	2881
2nd	DNN-best	10	32		tanh		0.25860	0.32917	20.07	9761
	DANN-best	3	256	7		poly	0.13784	0.16340	12.17	930817
	DANN-small	3	16	5		poly	0.24084	0.29161	24.84	3169
	HDANN1-best	5	1024	3	ReLU	poly	0.04920	0.05600	5.11	4218881
	HDANN1-small	7	16	3	ReLU	poly	0.22010	0.27233	15.97	1953
	HDANN2-best	5	1024	11	ReLU	poly	0.08971	0.14992	11.25	4216833
	HDANN2-small	3	64	7	ReLU	cos	0.24942	0.35515	13.10	9217
	HDANN3-best	7	256	7	tanh	cos	0.09411	0.15048	8.08	407553
	HDANN3-small	5	16	5	ReLU	poly	0.25859	0.35748	21.59	1665
3rd	DNN-best	8	128		tanh		0.29479	0.31256	13.11	116609
	DANN-best	3	256	7		poly	0.09222	0.12092	10.83	930817
	DANN-small	3	64	5		poly	0.15109	0.17232	14.12	43393
	HDANN1-best	9	1024	7	ReLU	poly	0.06996	0.08331	7.85	8441857
	HDANN1-small	5	16	7	ReLU	poly	0.24158	0.23220	14.32	1793
	HDANN2-best	3	1024	7	tanh	cos	0.15238	0.17052	10.33	2113537
	HDANN2-small	7	64	7	tanh	poly	0.23311	0.29389	17.37	25857
	HDANN3-best	9	64	11	ReLU	poly	0.10450	0.15059	19.83	38273
	HDANN3-small	7	16	9	tanh	poly	0.28260	0.26960	27.38	2657
4th	DNN-best	18	32		tanh		0.23065	0.23792	24.79	18209
	DANN-best	3	64	11		poly	0.11417	0.09610	20.11	95233
	DANN-small	3	16	7		poly	0.22674	0.17300	27.27	4417
	HDANN1-best	5	1024	3	ReLU	poly	0.04283	0.04475	5.51	4218881
	HDANN1-small	5	16	5	ReLU	poly	0.21227	0.26728	13.96	1601
	HDANN2-best	7	256	7	tanh	cos	0.12888	0.13913	9.53	398337
	HDANN2-small	5	64	7	tanh	cos	0.18766	0.23790	10.56	17537
	HDANN3-best	7	64	5	tanh	poly	0.09150	0.08640	15.00	27265
	HDANN3-small	5	16	7	tanh	poly	0.19589	0.15722	26.45	1889
5th	DNN-best	10	32		tanh		0.42048	0.33301	17.30	9761
	DANN-best	3	256	9		poly	0.13036	0.12474	10.02	1196545
	DANN-small	9	4	11		poly	0.34201	0.47686	71.27	1753
	HDANN1-best	9	1024	7	ReLU	poly	0.05554	0.05279	10.13	8441857
	HDANN1-small	3	16	7	ReLU	poly	0.32926	0.38209	13.85	1249
	HDANN2-best	5	1024	3	tanh	cos	0.13000	0.12084	12.00	4208641
	HDANN2-small	9	16	11	ReLU	cos	0.40186	0.42147	20.92	2465
	HDANN3-best	9	1024	7	ReLU	cos	0.10662	0.08755	10.71	8448001
	HDANN3-small	3	4	11	ReLU	cos	0.41798	0.37439	34.46	353

Table 6: Model 2 in scenario 2

Monte-Carlo sample	Network	L	p	q	σ	B_r	Validation Error	Test Error	Training Time (sec)	# of Parameters
1st	DNN-best	14	32		tanh		0.17844	0.23466	33.25	13985
	DANN-best	5	64	5		poly	0.07885	0.09495	16.08	84481
	DANN-small	3	16	5		poly	0.12545	0.18081	18.79	3169
	HDANN1-best	7	1024	5	ReLU	poly	0.03153	0.02817	5.26	6330369
	HDANN1-small	5	16	3	ReLU	poly	0.16609	0.22101	10.49	1409
	HDANN2-best	7	1024	3	ReLU	poly	0.05802	0.05988	7.84	6307841
	HDANN2-small	9	16	3	tanh	poly	0.17822	0.23816	38.32	2337
	HDANN3-best	7	1024	11	ReLU	cos	0.04894	0.06729	12.37	6377473
	HDANN3-small	5	16	3	ReLU	poly	0.17144	0.23110	18.03	1441
2nd	DNN-best	10	128		tanh		0.01934	0.02213	15.94	149633
	DANN-best	5	64	5		poly	0.01405	0.01593	19.47	84481
	DANN-small	5	16	5		poly	0.01778	0.02280	32.55	5761
	HDANN1-best	5	1024	7	ReLU	poly	0.01231	0.01224	5.04	4243457
	HDANN1-small	3	64	3	ReLU	poly	0.01657	0.02008	8.75	9601
	HDANN2-best	7	256	7	tanh	poly	0.01630	0.01592	17.84	398337
	HDANN2-small	5	256	3	ReLU	poly	0.01835	0.02421	11.27	265729
	HDANN3-best	9	64	3	tanh	poly	0.01351	0.01627	16.02	34689
	HDANN3-small	7	16	5	ReLU	poly	0.01933	0.02466	23.30	2209
3rd	DNN-best	14	128		tanh		0.02322	0.02022	20.64	215681
	DANN-best	3	64	11		poly	0.01450	0.01561	14.51	95233
	DANN-small	3	16	5		poly	0.02280	0.01997	18.80	3169
	HDANN1-best	7	1024	7	ReLU	poly	0.01202	0.01145	6.52	6342657
	HDANN1-small	7	16	5	ReLU	poly	0.02192	0.02014	13.64	2145
	HDANN2-best	7	256	3	tanh	poly	0.01808	0.01664	17.12	397313
	HDANN2-small	5	256	5	tanh	poly	0.02008	0.02010	18.50	266241
	HDANN3-best	9	256	5	ReLU	poly	0.01386	0.01253	9.38	535553
	HDANN3-small	5	16	7	ReLU	poly	0.02205	0.02160	17.55	1889
4th	DNN-best	12	128		tanh		0.02621	0.03349	16.05	182657
	DANN-best	3	256	5		poly	0.01407	0.01893	9.92	665089
	DANN-small	5	4	5		poly	0.02538	0.04560	66.62	481
	HDANN1-best	3	1024	7	ReLU	poly	0.01092	0.01428	3.66	2144257
	HDANN1-small	3	16	5	ReLU	poly	0.02571	0.03461	15.51	1057
	HDANN2-best	9	256	11	ReLU	poly	0.01743	0.02459	11.17	530945
	HDANN2-small	5	64	3	tanh	poly	0.02557	0.03313	28.10	17281
	HDANN3-best	7	64	5	ReLU	poly	0.01292	0.02142	12.78	27265
	HDANN3-small	7	4	9	ReLU	poly	0.02071	0.04186	40.39	377
5th	DNN-best	18	128		tanh		0.01702	0.02016	20.00	281729
	DANN-best	5	1024	5		poly	0.01498	0.01358	14.66	21012481
	DANN-small	3	1024	5		poly	0.01686	0.01564	13.91	10524673
	HDANN1-best	9	1024	5	tanh	poly	0.01326	0.01378	9.75	8429569
	HDANN1-small	7	64	3	tanh	poly	0.01428	0.01754	10.75	26241
	HDANN2-best	5	1024	7	ReLU	poly	0.01817	0.02410	10.61	4212737
	HDANN2-small	NA	NA	NA	NA	NA	NA	NA	NA	NA
	HDANN3-best	9	1024	11	ReLU	cos	0.01453	0.01370	14.04	8476673
	HDANN3-small	7	64	5	ReLU	poly	0.01606	0.01640	10.73	27265

7.3 Selected hyperparameters for Table 2

Fold(r)	Network	L	p	q	σ	B_r	Validation Error	Test Error	Training Time (sec)	# of Parameters
1st	DNN-best	8	2048		tanh		0.36354	0.36452	29.77	29394945
	DANN-best	3	256	3		cos	0.28369	0.29679	24.64	400897
	DANN-small	1	16	9		cos	0.34448	0.34292	47.59	1313
	HDANN1-best	5	256	9	tanh	cos	0.23888	0.25104	31.65	282113
	HDANN1-small	1	16	11	tanh	cos	0.35796	0.35257	38.75	1441
	HDANN2-best	7	256	7	ReLU	cos	0.26842	0.26609	29.61	398849
	HDANN2-small	5	16	9	ReLU	cos	0.36243	0.34882	47.86	1377
	HDANN3-best	9	256	11	tanh	cos	0.26357	0.27910	42.70	551937
	HDANN3-small	1	16	11	ReLU	cos	0.35315	0.34964	37.90	1873
2nd	DNN-best	10	512		tanh		0.35576	0.36719	35.76	2369025
	DANN-best	3	256	3		cos	0.28919	0.30267	35.17	400897
	DANN-small	1	16	9		cos	0.34481	0.35719	42.74	1313
	HDANN1-best	5	256	5	tanh	cos	0.24301	0.25160	45.46	273921
	HDANN1-small	7	4	11	ReLU	cos	0.34772	0.35618	91.18	481
	HDANN2-best	5	1024	3	ReLU	cos	0.26089	0.27114	26.28	4210689
	HDANN2-small	5	16	7	ReLU	cos	0.33417	0.35107	91.46	1345
	HDANN3-best	7	256	9	tanh	cos	0.27156	0.28325	43.75	415745
	HDANN3-small	1	16	9	ReLU	cos	0.35511	0.37081	55.81	1585
3rd	DNN-best	16	512		tanh		0.39892	0.41335	42.62	3944961
	DANN-best	5	256	3		cos	0.29730	0.30946	36.29	794625
	DANN-small	1	4	9		cos	0.39005	0.40920	57.34	329
	HDANN1-best	7	256	7	tanh	cos	0.25106	0.26462	40.85	409601
	HDANN1-small	3	4	9	tanh	cos	0.39860	0.41475	52.15	337
	HDANN2-best	7	1024	3	ReLU	poly	0.27795	0.29895	38.38	6309889
	HDANN2-small	7	16	7	ReLU	cos	0.38553	0.39270	72.36	1889
	HDANN3-best	9	256	7	tanh	cos	0.27094	0.28048	52.14	542721
	HDANN3-small	5	4	9	tanh	cos	0.38966	0.40568	60.28	409
4th	DNN-best	14	512		tanh		0.36918	0.35756	49.35	3419649
	DANN-best	5	64	3		cos	0.33428	0.32911	31.39	51201
	DANN-small	1	16	9		cos	0.35228	0.33861	57.29	1313
	HDANN1-best	5	256	7	tanh	cos	0.26450	0.25164	49.93	278017
	HDANN1-small	1	16	11	ReLU	cos	0.35975	0.34238	49.34	1441
	HDANN2-best	9	1024	3	ReLU	poly	0.30501	0.29238	31.69	8409089
	HDANN2-small	5	64	9	ReLU	cos	0.36121	0.35440	65.02	17793
	HDANN3-best	9	256	9	ReLU	cos	0.29437	0.28692	29.48	547329
	HDANN3-small	1	16	11	ReLU	cos	0.36017	0.34910	52.47	1873
5th	DNN-best	8	512		tanh		0.42504	0.41224	25.95	1843713
	DANN-best	3	64	3		cos	0.31279	0.31549	46.84	26497
	DANN-small	1	4	7		cos	0.39868	0.40350	41.10	257
	HDANN1-best	7	256	11	tanh	cos	0.23787	0.24019	57.01	417793
	HDANN1-small	3	4	7	ReLU	cos	0.41564	0.41419	55.44	273
	HDANN2-best	9	1024	11	ReLU	poly	0.30263	0.31050	46.30	8417281
	HDANN2-small	5	16	7	ReLU	cos	0.42393	0.42090	44.43	1345
	HDANN3-best	7	256	7	tanh	cos	0.26936	0.27074	41.00	411137
	HDANN3-small	1	4	9	ReLU	cos	0.41760	0.42425	51.06	349

References

- Bauer, B. and Kohler, M. (2019). On deep learning as a remedy for the curse of dimensionality in nonparametric regression. *Annals of Statistics*, **47**, 2261–2285.
- Bilodeau, M. (1992). Fourier smoother and additive models. *Canadian Journal of Statistics*, **20**, 241–351.
- Cybenko, G. (1989). Approximation by superpositions of a sigmoidal function. *Mathematics of Control, Signals, and Systems*, **2**, 303–314.
- Fakhoury, D., Fakhoury, E. and Speleers, H. (2022). ExSpliNet: An interpretable and expressive spline-based neural network. *Neural Networks*, **152**, 332–346.
- Glorot, X. and Bengio, Y. (2010). Understanding the difficulty of training deep feedforward neural networks. *AISTATS*, **9**, 249–256.
- Haar, A. (1910). Zur Theorie der orthogonalen Funktionensysteme. *Mathematische Annalen*, **69**, 331–371.
- Horowitz, J. L. and Mammen, E. (2007). Rate-optimal estimation for a general class of nonparametric regression models with unknown link functions. *Annals of Statistics*, **35**, 2589–2619.
- Jeon, J. M. and Park, B. U. (2020). Additive regression with Hilbertian responses. *Annals of Statistics*, **48**, 2671–2697.
- Jeon, J. M., Lee, Y. K., Mammen, E. and Park, B. U. (2022). Locally polynomial Hilbertian additive regression. *Bernoulli*, **28**, 2034–2066.
- Kidger, P. and Lyons, T. (2020). Universal Approximation with Deep Narrow Networks. *Proceedings of Machine Learning Research*, **125**, 1–22.
- Kingma, D. P. and Ba, J. M. (2017). Adam: A Method for Stochastic Optimization. *arXiv:1412.6980v9*.
- Kohler, M. and Langer, S. (2021). On the rate of convergence of fully connected deep neural network regression estimates. *Annals of Statistics*, **49**, 2231–2249.

- Kolmogorov, A. N. (1957). On the representation of continuous functions of many variables by superposition of continuous functions of one variable and addition. *Doklady Akademii Nauk SSSR*, **114**, 953–956.
- LeCun, Y., Bengio, Y. and Hinton, G. (2015). Deep learning. *Nature*, **521**, 436–444.
- Linton, O. and Nielsen, J. P. (1995). A kernel method of estimating structured nonparametric regression based on marginal integration. *Biometrika*, **82**, 93–101.
- Liu, Z., Wang, Y., Vaidya, S., Ruehle, F., Halverson, J., Soljačić, M., Hou, T. Y. and Tegmark, M. (2024). KAN: Kolmogorov-Arnold Networks. [arXiv:2404.19756v4](https://arxiv.org/abs/2404.19756v4).
- Mammen, E., Linton, O. B. and Nielsen, J. P. (1999). The existence and asymptotic properties of a backfitting projection algorithm under weak conditions. *Annals of Statistics*, **27**, 1443–1490.
- McLaughlin, J. R. (1969). Haar Series. *Transactions of the American Mathematical Society*, **137**, 153–176.
- Meier, L., van de Geer, S. and Bühlmann, P. (2009). High-dimensional additive modeling. *Annals of Statistics*, **37**, 3779–3821.
- Opsomer, J. D. and Ruppert, D. (1997). Fitting a bivariate additive model by local polynomial regression. *Annals of Statistics*, **25**, 186–211.
- Pereyra, M. C. and Ward, L. A. (2012). *Harmonic Analysis: From Fourier to Wavelets*. American Mathematical Society.
- Sardy, S. and Ma, X. (2024). Sparse additive models in high dimensions with wavelets. *Scandinavian Journal of Statistics*, **51**, 89–108.
- Schmidt-Hieber, J. (2020). Nonparametric regression using deep neural networks with ReLU activation function. *Annals of Statistics*, **48**, 1875–1897.
- Schmidhuber, J. (2015). Deep learning in neural networks: An overview. *Neural Networks*, **61**, 85–117.